Chapter 4

Circulation in the Gulf of Aden

4.1 Introduction

As described in Chapter 1 the winds over the north Indian Ocean and Gulf of Aden reverse their direction from summer to winter owing to monsoons. Over the Gulf of Aden and the northwestern Arabian Sea, the winter monsoon sets in from November and persists till March (Figure 1.2). The summer monsoon sets in towards the end of May over the Gulf of Aden, shortly after it is established over the western Arabian Sea (Figure 1.2). During this season, over the gulf, the wind speed increases rapidly from ~ 6 m s^{-1} in the west to $\sim$17 m s^{-1} in the east and adjoining northwestern Arabian Sea. October represents the transition between the summer to winter monsoons and April–May (first half of May) represents the transition between winter to summer. The winds are much stronger during the summer monsoon than those during the winter monsoon. These seasonally reversing monsoonal winds over the Arabian Sea and Gulf of Aden force a seasonally reversing circulation in the surface layer. The best studied seasonally reversing current in the northwestern Arabian Sea, the Somali Current, flows poleward (equator ward) along the coast of Somalia during the summer (winter) monsoon (see the reviews by Schott [1983]; Shetye and Gouveia [1998]; Schott and McCreary [2001]). Owing to the reversal

of winds, the surface currents in the Gulf of Aden also reverse seasonally.

From the available literature, it appears that very few attempts have been made to study the circulation in the Gulf of Aden. Due to the lack of published literature, in peer reviewed journals, we have to depend, mainly, on the unpublished articles. In one such article, Kolli et al. [1992] presented a preliminary analysis of the surface currents in the Gulf of Aden based on ship drifts and limited hydrographic observations. Wooster et al. [1967] stated that the winter pattern starts in October with a weak westward flow into the gulf. It developed fully in November and persisted till April . During summer, the direction of the surface current reversed with an increased strength. An anticyclonic eddy also appeared in the center during July–August (see charts no. CA1-CA4 of Wooster et al. [1967]).

The dynamic topography maps prepared by Wyrtki [1971] indicated weak northeasterly flows along the northeastern part of Gulf of Aden during January–February. During the summer monsoon period (July–August), an anticyclonic eddy formed in the center of the gulf, and shifted eastward towards the mouth of the gulf during September–October. The dynamic topography maps of Seriy and Khimitsa [1963] indicated two eddies in the Gulf of Aden during the winter monsoon, one cyclonic in the gulf, east of 50° E, and the other anticyclonic to the east of the gulf off Ras Fartak.

Mohammed and Kolli [1992] used the hydrographic data from three cruises to describe the circulation in the northern Gulf of Aden. During January, one cyclonic eddy developed between 46° E and 50° E. West of the cyclonic eddy, the flow was towards Bab el Mandab. During May, the flow was generally weak with an anticyclonic eddy in the eastern gulf. During August, an anticyclonic eddy appeared in the center of the gulf and another near the eastern end of the gulf between 50° E and 52° E.

Murray and Johns [1997] studied the exchange between the Red Sea and the Gulf of Aden and found that it is strongly seasonal due to the influence of monsoon winds and due to the variations in buoyancy fluxes; the maximum outflow of RSW (0.6 Sv) occurred

during winter and the minimum (0.05 Sv) during summer. Recent observations of Bower et al. [2002, 2005] revealed the spreading of RSW influenced by a chain of deep–reaching mesoscale eddies. The exchange between the Gulf of Aden and the Somali current system occurs mainly through the Socotra Passage [Schott and Fischer, 2000].

Though the aforementioned studies gave a preliminary description of the seasonal behaviour of surface currents in the Gulf of Aden, they could not provide a detailed description of the monthly evolution of circulation in the Gulf of Aden. Similarly, most of these studies covered only the northern part of the gulf due to the paucity of data along the southern part. Thus there is a controversy among them on the characteristics of eddies and their role in the circulation. For example, the dynamic topography maps of Wyrtki [1971] during January–February indicated a northeasterly flow along the northeastern part of the gulf; while Mohammed and Kolli [1992] showed a cyclonic cell between 46 and 50° E indicating a westward flow along the northern side of the gulf. Also they could not establish the influence of eddies on the circulation at the surface or in the deeper layers.

To describe the surface circulation in the Gulf of Aden, we have used four different datasets: (i) ship drift data to get an overall idea of the circulation in the gulf, (ii) the QuikSCAT winds (described in Chapter 2) to estimate the surface Ekman drift, (iii) the hydrographic data (described in Chapter 2) and satellite altimeter derived sea level anomaly (SLA) (also described in Chapter 2) to estimate the geostrophic currents. The net surface currents resulting from Ekman drifts and geostrophic currents were then used to describe the surface circulation. The geostrophic current derived from hydrographic data was first compared with the geostrophic currents derived from altimeter and then used to describe the circulation in the deeper region of the Gulf of Aden.

Figure 4.1 The surface currents derived from ship drifts (cm s^{-1}). The source for the ship drifts is the Ocean Current Drifter Data CDROMs NODC-53 and NODC-54 (NODC, Department of Commerce, NOAA).

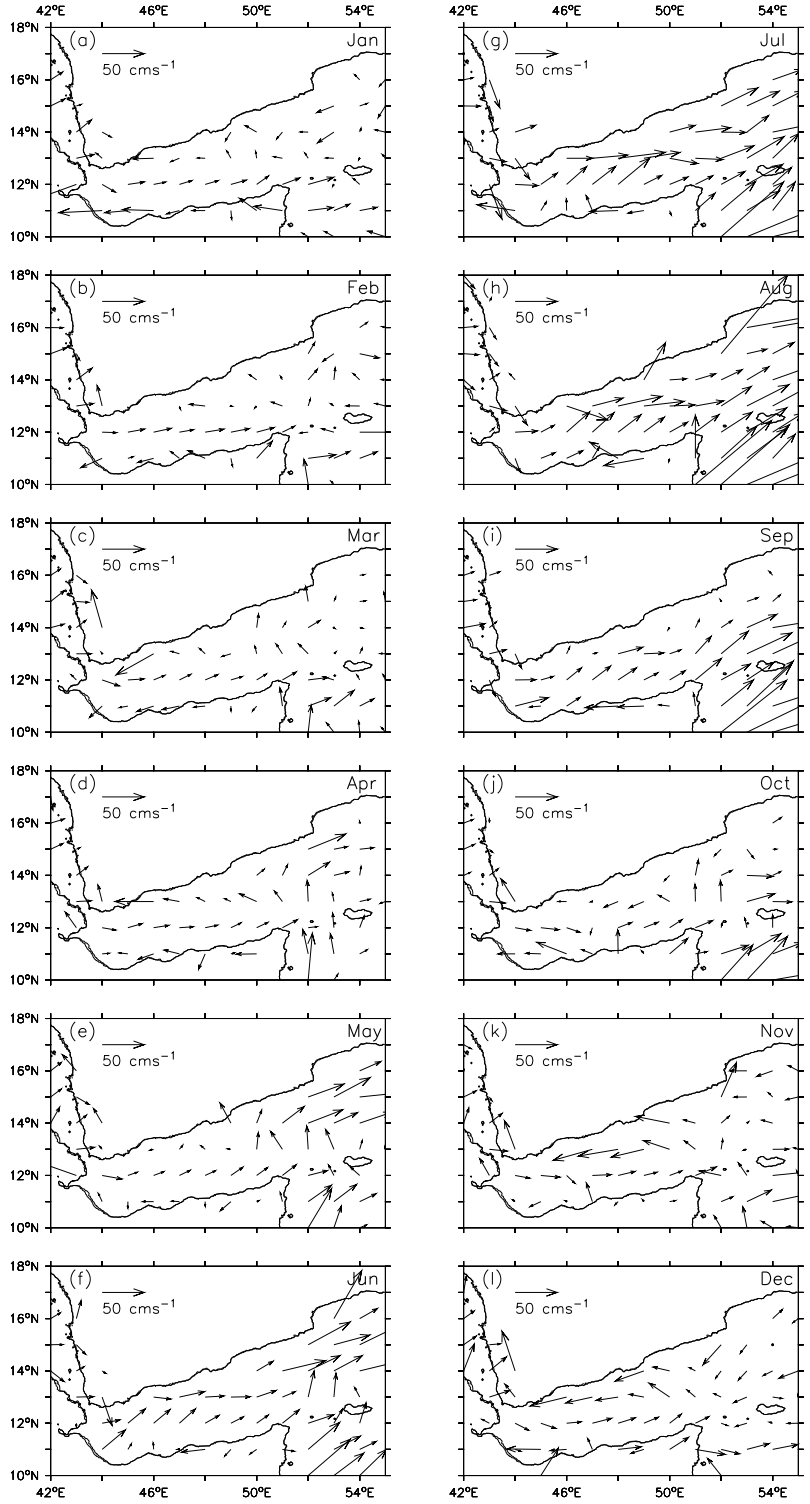

4.2 Surface currents

4.2.1 Ship drifts

Before the days of satellite–tracked floats and buoys and satellite-based altimeters and scatterometers, scientists relied on ship drift data to map the surface currents in the oceans. Here we have used the monthly climatology of ship drifts available from the National Oceanographic Data Center (NODC), NOAA on a spatial resolution of 1° longitude x 1° latitude to describe the surface circulation in the Gulf of Aden. Figure 4.1 shows the monthly climatology of ship drifts over the Gulf of Aden.

In November, a typical winter month, westward flows are observed in the northern gulf and eastward flows are observed in the mid and southern gulf. The flows along the southern coast are weak; eastward in the east (east of 48° E) and westward in the west (west of 45° E). The westward flow in the northern gulf appears to be stronger than the eastward flow. Similar patterns continue in December. The magnitude of the westward flow in December is $\sim$ 30 cm s^{-1} whereas the eastward flow in the south is about 20 cm s^{-1} (Figure 4.1l). During January–March the flows continue to follow the same pattern with a westward flow along the northern side and an eastward flow in the middle. However, during these months, the traces of weak westward flow seen in November–December along the southern coast extend all along the coast. In April–May, the pattern continues but with weaker magnitudes (Figure 4.1d, and e).

In June when the summer monsoon establishes over the gulf, flows along the northern and southern boundaries undergo a complete reversal. The eastward flows get established all over the gulf during June–September. Their magnitude peaks in July–August to 40–50 cm s^{-1} (Figure 4.1g and h). During this period, the flows outside the gulf, in the adjacent northwestern Arabian Sea, are stronger than that inside the gulf. In October, the period of transition from summer to winter, the flows diminish and reverse direction along the northern and southern coasts (Figure 4.1j).

In summary, the ship drifts clearly capture the annual cycle of reversing surface currents in the Gulf of Aden. During the summer monsoon, a strong eastward current is established all over the gulf. Whereas during the winter monsoon the westward currents are seen along the northern and southern coasts with eastward flows in the middle.

4.2.2 Ekman Drift

Wind stress is communicated to the ocean surface layer through viscous (frictional) processes that extend several tens of meters into the ocean. For time scales longer than inertial periods, the response is strongly affected by Coriolis acceleration. This wind–driven frictional layer is called the "Ekman layer". The wind drag acting on the Ekman layer tries to push the water in the direction of the wind, but the Coriolis force, which is the only other force involved, must balance the wind drag therefore must be equal in magnitude but opposite to the wind drag. The net effect of these two forces deflects the surface currents at 45° to the right (left) of the wind in the northern (southern) hemisphere. Such currents arising due to the direct effect of winds at the surface are called Ekman drifts.

The surface Ekman drift was computed using the Ekman spiral method described in Pond and Pickard [1983]. Following this method, the zonal (u) and meridional (v) velocities were estimated as:

$$u = \frac{\tau_x}{\rho_0\sqrt{A|f|}}\sin(45) + \frac{\tau_y}{\rho_0\sqrt{A|f|}}\cos(45) \tag{4.1}$$

$$v = -\frac{\tau_x}{\rho_0\sqrt{A|f|}}\cos(45) + \frac{\tau_y}{\rho_0\sqrt{A|f|}}\sin(45) \tag{4.2}$$

where τ_x, τ_y are the magnitudes of the wind stress in zonal and meridional directions respectively, A is the vertical eddy diffusivity, ρ_0 is the average density of seawater, and $|f|$ is the magnitude of the Coriolis parameter. We used $A = 10^{-2}m^2s^{-1}$ [Hastenrath and Greischar, 1991].

Figure 4.2 Climatology of surface Ekman drifts (cm s^{-1}) in the Gulf of Aden and northwestern Arabian Sea. The Ekman drift was estimated using the QuikSCAT wind climatology for the period 1999-2006.

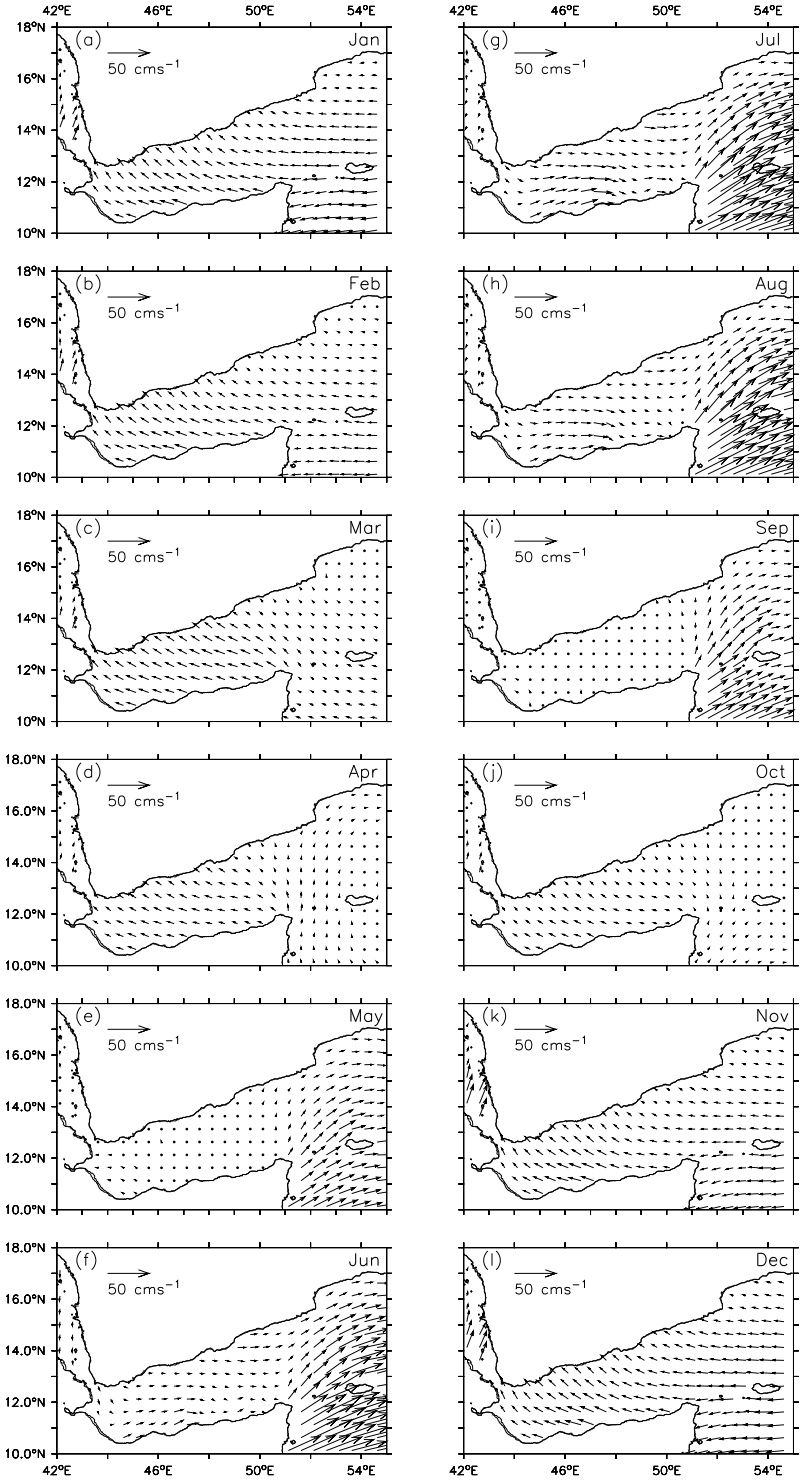

Figure 4.2 shows the climatology of surface Ekman drift over the Gulf of Aden and adjoining northwestern Arabian Sea estimated using the QuikSCAT wind climatology for the period 1999–2006. In November, when the winter monsoon establishes over the gulf, the Ekman drift in the Gulf of Aden and the adjacent northwestern Arabian Sea is towards the west. The winter monsoon peaks in December–January with northeasterly winds over the Arabian Sea and Gulf of Aden. The associated westward Ekman drift also strengthens (~ 20 cm s^{-1}). It is westward over the eastern gulf (east of 48° E) and the adjacent northwestern Arabian Sea but veers towards the northwest over the western gulf (west of 48° E). This winter monsoon pattern continues till February–March over the northwestern Arabian Sea and till April over the gulf but with weaker magnitude. In fact, the westward drift, though weaker (< 10 cm s^{-1}) , starts in October (Figure 4.2j) before the establishment of winter monsoon winds over the gulf and adjacent Arabian Sea. Hence, in general, the winter pattern of Ekman drift (westward drift) sets over the gulf in October and continues till April.

The summer monsoon sets over the northwestern Arabian Sea towards the end of May with southwesterly winds and strong Ekman drifts towards the northeast (20 cm s^{-1}). But the Ekman drifts over the gulf remain weak (< 5 cm s^{-1}) due to weak winds (Figure 4.2e). The summer monsoon pattern strengthens during June over the Arabian Sea as well as over the gulf (Figure 4.2f). Over the gulf, the eastward drift has a magnitude $\sim$ 15 cm s^{-1} , when the northeastward drift is much stronger (~ 40 cm s^{-1}) over the northwestern Arabian Sea. In July–August, the peak of the summer monsoon, eastward Ekman drifts reach ~ 20 cm s^{-1} over the gulf and ~ 80 cm s^{-1} over the adjacent northwestern Arabian Sea. Similar drift magnitudes were observed earlier [Shankar et al., 2002] using Hellerman and Rosenstein [1983] wind stress also. The summer monsoon pattern vanishes over the gulf in September though it continues to prevail over the northwestern Arabian Sea (Figure 4.2i).

During the summer monsoon, Ekman drift over the Gulf of Aden is weaker than that

over the northwestern Arabian sea. The Ekman drift over the gulf is favourable for upwelling along the northern coast during summer monsoon and it is favourable for upwelling along the southern coast during the winter monsoon.

In summary, similar to ship drifts, the Ekman drifts over the Gulf of Aden undergo a complete reversal in response to the reversing monsoonal winds. However, unlike the ship drifts, the Ekman drifts are unidirectional all over the gulf.

4.2.3 Geostrophic Currents

In the oceans at time scales longer than several days and at spatial scales longer than several kilometers, the balance of forces in the horizontal is between the pressure gradient force and the Coriolis force. This is called "geostrophic balance" or geostrophy. When the flow is geostrophic, forces and accelerations other than the pressure gradient and Coriolis force become negligible . Under geostrophic balance, the pressure gradient forces the water parcel to move from high to low pressure, but Coriolis force moves the parcel off to the right (left) in the northern (southern) hemisphere. In a steady geostrophic state, the water parcel moves exactly perpendicular to the pressure gradient force. The vertical force balance that always goes with geostrophy is hydrostatic balance. The vertical pressure gradient force, that points upwards from high pressure to low pressure, is balanced by gravity, that points downward.

The mathematical expression for the geostrophy is

$$-fv = -\frac{1}{\rho_0}\frac{\partial P}{\partial x} \tag{4.3}$$

$$fu = -\frac{1}{\rho_0}\frac{\partial P}{\partial y} \tag{4.4}$$

and the hydrostatic balance is

$$0 = -\frac{\partial P}{\partial z} - \rho g \tag{4.5}$$

Here f is the Coriolis parameter, u,v are the components of the horizontal velocity, ρ and ρ_0 are the density and a constant reference value respectively, x, y, z denote Cartesian coordinates with z oriented upward, and P is the pressure.

In this study, we have estimated the geostrophic currents using two datasets, a satellite bound altimeter derived sea level anomaly and a climatology of hydrography (1923-2005). The detailed descriptions of the data sets are available in Chapter 2. The motion is assumed to be zero at 1000 m level (level of no motion) for the purpose of geostrophic computation using hydrographic data. The merged altimeter data (TOPEX/Poseidon, ERS-1/2), available in the spatial resolution of 0.3° x 0.3° degrees at weekly intervals for 11 years (1993–2003) is used to construct the monthly climatology of sea level anomaly. The sea level anomaly is then used to compute the geostrophic currents following

$$u = -\frac{g}{f\rho}\frac{\partial \eta}{\partial y} \tag{4.6}$$

$$v = \frac{g}{f\rho}\frac{\partial \eta}{\partial x}, \tag{4.7}$$

To derive the geostrophic currents (relative to 1000 m level) from hydrographic data set, first a monthly climatology of the available hydrographic data (temperature and salinity spanned over a period of 82 years during 1923–2005) was prepared on 0.5° longitude x 0.5° latitude spatial grids as described in Chapter 2. The monthly climatology was then used to derive the geostrophic currents following the procedure detailed in Pond and Pickard [1983].

The surface geostrophic currents derived from both data sets, altimeter SLA and hydrography, are shown in (Figure 4.3). The region west of 45° E is not covered by the hydrography derived geostrophic currents, because the currents are estimated with reference to 1000 m and the region west of 45° E is shallower than 1000 m. Unlike the

ship and Ekman drifts, the geostrophic currents show large spatial variations; often they are dominated by cyclonic and anticyclonic eddies. In Figure 4.3, the locations of these eddies are marked as C (cyclonic) and A (anticyclonic).

The geostrophic currents derived from the hydrographic data and from the altimeter SLA , show similar patterns over the Gulf of Aden. Prior to the establishment of winter, in October, the geostrophic currents derived from both data sets (Figure 4.3j) show the dominance of 3 eddies; an anticyclonic eddy (A1 at 52° E) in the east and two cyclonic eddies (C1 at 48° E and C2 at 45.5° E) inside the gulf. The C1 and C2 eddies are separated by a distance of $\sim$ 150 km in both data sets. In November, the western most eddy C2 disappears and C1 appears further west (47° E) but as a larger eddy covering most of the gulf (Figure 4.3k). The expansion of C1 eddy prompts westward currents along the northern coast and eastward currents along the southern coast. The magnitude of these currents along the northern and southern boundaries are $\sim$ 20–30 cm s^{-1}. The A1 eddy also moves further west (51.5° E) as seen in altimeter SLA, but is not seen clearly in the hydrographic data. As the eddy A1 moves towards the west, another cyclonic eddy C3 appears outside the gulf at 54° E. This eddy is seen in both data sets. The November pattern repeats in December and January except for the apparent shift of eddies C1, A1 and C3. Also, a new anticyclonic eddy (A2) appears in the east, just outside the gulf, between the longitudes 52.5° E and 54.5° E (Figure 4.3l and a). The eddy (A2) is seen in the hydrographic data in December and in the altimeter SLA in January. However, the strength of the currents diminishes ($\sim$ 20 cm s^{-1}) in January than that in November–December. The strength of the geostrophic currents further diminishes in February ($\sim$ 10–15 cm s^{-1}) though the eddies continue to dominate the flow field (Figure 4.3b). All eddies (C1, C3, A1 and A2) seen during November to January continue to exist with less vigour. The eddy pattern dominates the flow field in March–April with weaker geostrophic currents ($\sim$ 10 cm s^{-1}). The C1 eddy seen in March is not seen in April. All other eddies A1, C3 and A2 are seen with a westward shift. Alternate cyclonic and anticyclonic eddies force a

meandering flow pattern in March.

The eddy field strengthens again in May (Figure 4.3e). The altimeter SLA shows three anticyclonic eddies in a row, two inside the gulf (A1 and A3) and one in the east of the gulf (A2). But the hydrographic data shows a cyclonic eddy (C1) inside the gulf in the west in place of A1 in the altimeter SLA.

In June, when the summer monsoon becomes active over the gulf and adjoining north-western Arabian Sea, the eddy fieled also gets strengthened further. An anticyclonic eddy dominates the entire gulf; it appears as a large single eddy in the altimeter SLA derived geostrophy and as two anticyclonic eddies (A1 and A3) in hydrography. Also another anticyclonic eddy (A2) is seen outside the gulf at 54° E in both data sets. The altimeter SLA derived geostrophy also shows a cyclonic eddy extending towards the gulf from the Somali coast, but not clear (C4) in the hydrography due to the absence of data in that region. The geostrophic currents associated with the anticyclonic eddy inside the gulf are towards the east along the northern coast and towards the west along the southern coast.

The anticyclonic eddy (A1) inside the gulf strengthens further in July and the magnitude of associated eastward currents along the northern coast exceeds 50–60 cm s^{-1}. But the size of the eddy reduces than that in June. The cyclonic eddy (C4) extends further north touching the northern coast of the gulf. Due to the presence of this cyclonic eddy, the eastward flows along the northern coast deflect southeastwards when they arrive at the western flank of the cyclonic eddy (Figure 4.3g). The anticyclonic eddy seen outside the gulf strengthens further in both data sets.

In August, the anticyclonic eddy (A1) shrinks further and weakens leading to the weakening of associated geostrophic currents ($\sim$ 40 cm s^{-1}). Also, the cyclonic eddy C4 seen in the east of A1 expands towards the west as well as towards the east along the northern coast. The sea level also drops (by about 10 cm) in the west of A1 in both data sets; but the drop in sea level has not manifested as a cyclonic eddy. The existence of low sea level interspaced with high sea level (A1) manifests as a meandering eastward flow in

Figure 4.3 Geostrophic currents (cm s^{-1}) at surface derived from the monthly climatology of hydrography (left panels) and altimeter derived SLA (right panels). The colour shades on the left panels represents the dynamic topography (dyn cm) (0/1000) and the colour shades on the right panels show the SLA (cm). The basin–wide mean (147 dyn cm) is removed from the dynamic topography field to represent the dynamic topography and SLA in same scale. C(A) denotes cyclonic (anticyclonic) eddy.

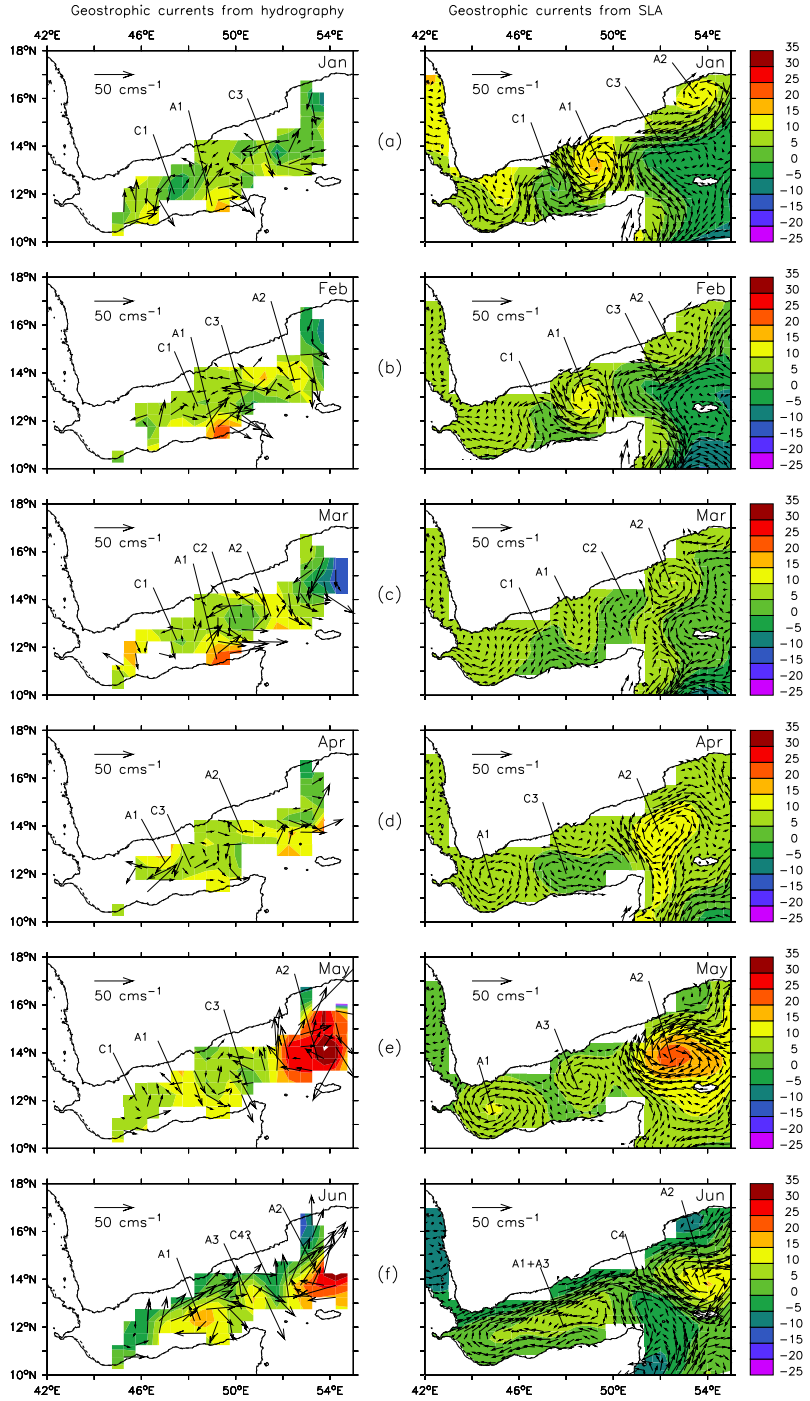

Figure 4.3 (Continued)

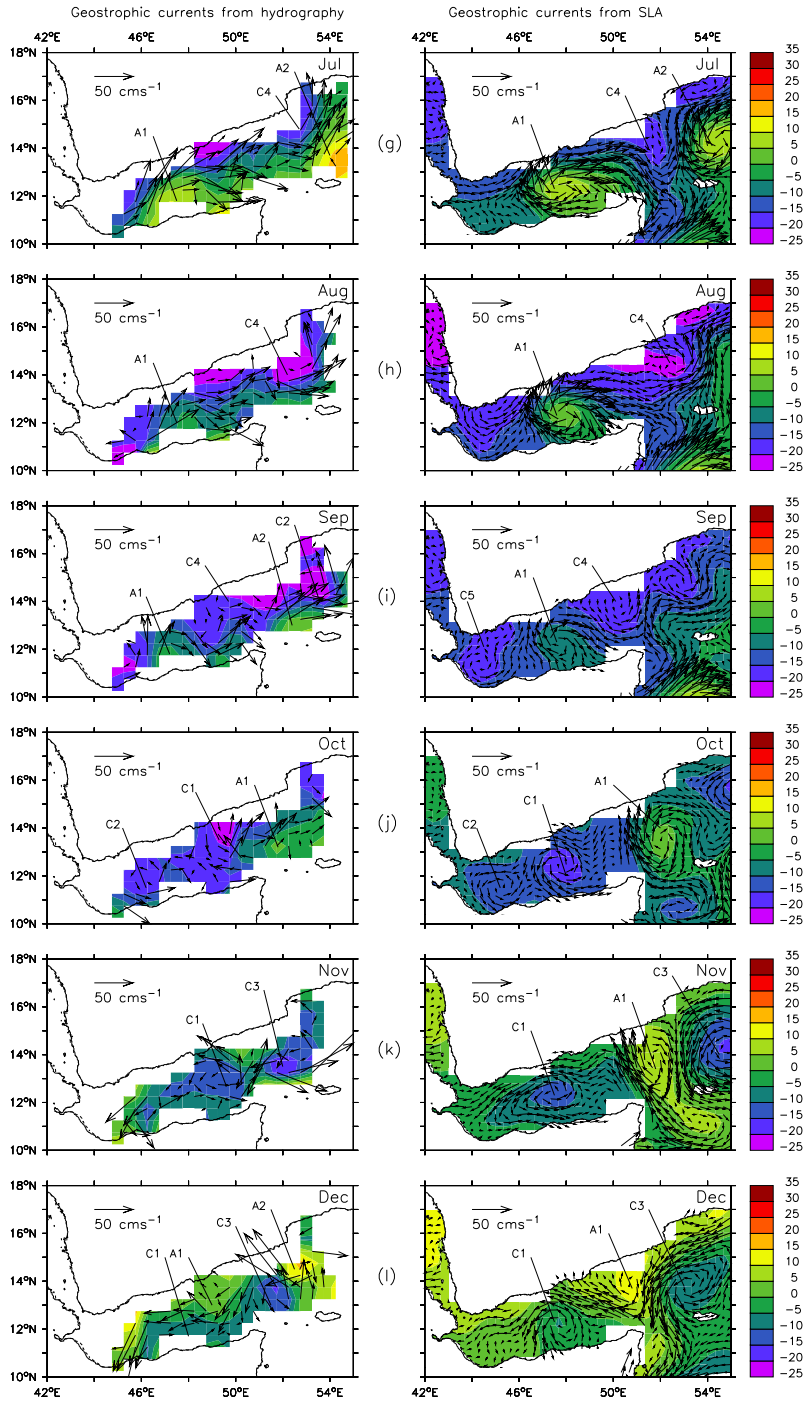

the Gulf of Aden (Figure 4.3h). A similar situation prevails in September also but with weaker geostrophic velocities. The anticyclonic eddy A1, seems to have shifted towards the west from its position at 48° E to 47.5° E. Similarly, the core of the cyclonic eddy, C4 also seems to have shifted towards the west from 52° E to 50.5° E.

In summary, the geostrophic currents in the Gulf of Aden are composed of several cyclonic and anticyclonic eddies and the flow directions along the coasts change depending on the type of eddy that appears in its vicinity. More eddies are seen during winter than in summer, but the geostrophic flows reach their peak in the summer monsoon season in July. The geostrophic currents derived from the altimeter SLA and the hydrography seem to be in good agreement with each other. The type of eddies, their position etc match well in both data sets. The magnitude of geostrophic velocities derived from the altimeter derived SLA, however, cannot be compared with those derived from hydrography because the geostrophic velocities estimated from the hydrographic data are relative to the level of no motion (in this case 1000 m level).

The good match between the geostrophic currents at the surface derived from altimeter derived SLA and hydrography allow us to use either of them to describe the net currents at the surface (geostrophy+Ekman). To derive the net currents at the surface of the Gulf of Aden we chose to use the altimeter SLA derived geostrophic currents and the Ekman drifts presented in 4.2.2. The choice of altimeter SLA derived geostrophic currents over the hydrography derived is made because of its better spatial coverage and resolution.

Similarly, the good match between the geostrophic currents derived from altimeter measured SLA and hydrography gives confidence in using hydrography to describe the geostrophic currents in the deeper layers. Hence, we have used the geostrophic currents derived from hydrography to describe the circulation in the deeper layers.

4.2.4 Net surface currents in the Gulf of Aden

The net flows at the surface of the Gulf of Aden (the sum of Ekman drift and geostrophic current derived from altimeter SLA) are shown in Figure 4.4.

During the transition between summer and winter monsoons, in the month of October, the net surface flows in the gulf are punctuated with three well marked eddies; two cyclonic (C1 and C2) and an anticyclonic (A1) at the entrance to the gulf (Figure 4.4j) as seen in the geostrophic flows (Figure 4.3j). Clearly, during October, the flows are primarily geostrophic all over the gulf with westward flows along the northern boundary and weak eastward flows along the southern boundary (Figure 4.4j). The westward flow continues towards the Red Sea through Bab el Mandab. Near the entrance of the gulf, between C2 and A1, the flows are towards the west contributed by both geostrophy and Ekman drift. The azimuthal velocities in the anticyclonic eddy (A1) are $\sim$ 30–40 cm s^{-1}.

In November when the winter monsoon establishes over the Gulf of Aden and the northwestern Arabian Sea, the eddy C2 disappears and the eddies C1 and A1 appear further west from their October positions. Another cyclonic eddy (C3) appears east of A1 in the northwestern Arabian Sea. Inside the gulf, the strong westward flows get established in the northern part of the gulf due to the strengthening of Ekman drift while the eastward flow along the southern part is weak (Figure 4.4k). The surface flow towards the Red Sea strengthened during this month. In the east, the flows strengthen as northwestward flows along the western flank of A1.

The westward flow inside the gulf strengthens during December and the eddies shrink considerably. The eddy C1 is squeezed towards the south and A1 towards the north (Figure 4.4l) due to the strengthening of westward Ekman drift (Figure 4.2l). The flow towards the Red Sea through the Bab el Mandab also strengthens. The flow entering the gulf from the northwestern Arabian Sea is strong and towards the southwest.

During January and February, as the westward flows continue inside the gulf, the anticyclonic eddy (A1) gets better organised at 49° E. (Figure 4.4a). At the western most

part of the gulf, near the Bab el Mandab, the flows are northwestward towards the Red Sea. In the east, at the entrance to the gulf, under the influence of the anticyclonic eddy, strong westward flows are seen in the northern half and weak southeastward flows are seen in the southern half. Outside the gulf, in the northwestern Arabian Sea, the flow is similar to that in December. Along the Arabian coast another anticyclonic eddy (A2) is seen between 53° E and 55° E.

In March–April, the transition between the winter monsoon and the summer monsoon, the geostrophic currents weaken inside the gulf and the Ekman drifts dominate the westward flows (Figure 4.4c and d). The westward flow towards the Red Sea continues during these months also. The anticyclonic eddy (A1) seen during January–February is not seen in March, but appears as a weakly formed eddy in April. Near the entrance, the northeasterly geostrophic flow is modified by the westward Ekman drift. The anticyclonic eddy (A2) which appeared in January–February near the Arabian coast is well formed and shifts towards the southwest.

The month of May is punctuated by a row of three anticyclonic eddies, A1, A3 and A2. It is not clear whether A3 was a new formation or the manifestation of A2 that moved westward. In that case, the eddy marked as A2 in Figure 4.4e will not be the same eddy as that seen in March–April. At this stage, we will not go into the details of these eddies because Chapter 5 describes them in detail. The flows during this month are eddy centric; eastward flows along the northern coast with a discontinuity at 47.5° E and westward flows along the southern coast with a discontinuity at 48° E. May is the month of the pre–summer monsoon, which means the geostrophic currents dominate with eastward flows along the northern side and westward currents along the southern side of the gulf. In the east, near the entrance, the flows are either northward or northwestward under the influence of anticyclonic eddy (A2). Outside the gulf in the northwestern Arabian Sea the flows have strengthened ($\sim$ 30–40 cm s^{-1}) due to the strengthening of Ekman drift.

In June when the summer monsoon establishes over the Gulf of Aden and the north-

Figure 4.4 Net surface flow (cm s^{-1}) computed as the sum of Ekman drift (Figure 4.2) and geostrophic currents at the surface derived from SLA (Figure 4.3).

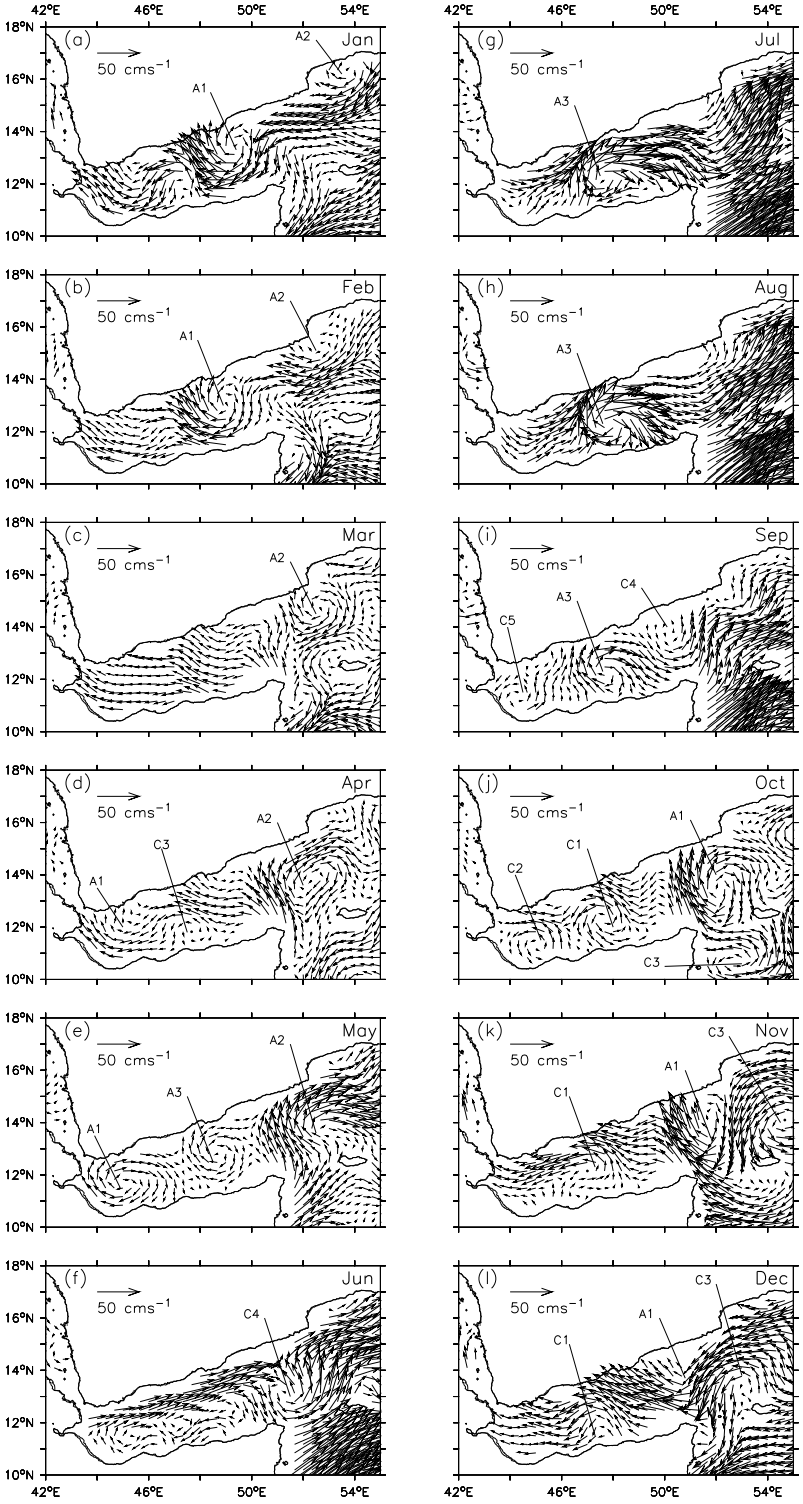

western Arabian Sea, strong eastward (30–40 cm s^{-1}) flows develop in the northern half of the gulf. In the southern half, the westward flows embedded with micro-eddies (not particularly identified) are weak (Figure 4.4f) due to the eastward Ekman drifts (Figure 4.2f) and the weak geostrophic currents (Figure 4.3f). At the entrance of the gulf, a cyclonic eddy (C4) is seen. That seems to be due to the combination of Ekman drift and geostrophy.

During July–August, the summer monsoon strengthens the associated surface flows dominated by the Ekman drift. Over the gulf, by and large, the flows are toward the east, except in the middle where the anticyclonic eddy (A3) generates a westward flow along the southern coast. The azimuthal velocities of A3 are in the range of $\sim$ 40–60 cm s^{-1} (Figure 4.4g and h). In the northwestern Arabian Sea, the northeasterly flows have the magnitude $\sim$ 80 cm s^{-1}.

During September the net surface flows weaken considerably, due to weak Ekman drifts inside the Gulf of Aden. As a result, the geostrophic currents (a row of three eddies C5, A3 and C4) dominate the flows inside the gulf (Figure 4.4i). However, the azimuthal velocities of eddy, A3 are weaker ($\sim$ 30–40 cm s^{-1}) than those in July–August. In the northwestern Arabian Sea, the flows continue in the northeasterly direction (Figure 4.4i) as those in July–August.

In general, during winter, the net flows are towards the west over most of the gulf with cyclonic and anticyclonic eddies embedded in it. This flow structure establishes in October and continues till April, mostly dominated by geostrophy. In May also, the geostrophy dominates the net surface flows because of weak Ekman drifts. During June, at the beginning of the summer monsoon, the flows are eastward in the northern half of the gulf and are westward along the southern half, whereas during the rest of summer monsoon, the flows are eastward all over the gulf.

4.3 Vertical structure of geostrophic currents

As discussed earlier, the geostrophic velocity derived from hydrgraphic data is used to describe the currents at two depth levels, 300 and 600 m. Also described is the vertical structure (from surface to 1000 m) of geostrophic currents across a section in the middle of the Gulf of Aden. For easy comparison, the geostrophic currents at the surface are also shown in Figure 4.5. The two depth levels 300 and 600 m are chosen because the core of Gulf of Aden Intermediate Water flows, more or less, at 300 m level and the core of Red Sea Water flows at around 600 m depth level (see Chapter 3 for a detailed description of water masses in the Gulf of Aden).

During October (Figure 4.5j) the geostrophic currents at 300 m and 600 m are punctuated with three eddies, two cyclonic (C1 and C2) and an anticyclonic similar to those at the surface. The westward flow along the northern side of the gulf and eastward flow along the southern side at 300 and 600 m seem to be similar to that at the surface. The geostrophic currents across the vertical section along the center of the gulf, shown in the bottom panel of Figure 4.5j, also confirm the penetration of eddies up to 1000 m.

In November, the westward flows along the northern side at the surface are repeated at 300 and 600 m. So are the cyclonic eddies C1 and C3 (Figure 4.5k). However, in addition to those two cyclonic eddies an anticyclonic eddy (A1) is also seen in the south central gulf at 300 and 600 m. The vertical section of geostrophic velocities shown in the bottom panel confirms the presence of cyclonic eddies to 1000 m.

In December, the westward currents are strong in the northern half of the gulf, but weaken at 300 and 600 m. However, the signature of the eddies seen at the surface are seen at both levels (Figure 4.5k). The banding structure of geostrophic currents shown in the vertical section (bottom panel) reaches as deep as 1000 m.

During January–March also, there are a row of eddies at the surface as well as in the deeper layers. The anticyclonic eddy, A1, is better developed in January than the cyclonic eddies C1 and C3. The cyclonic eddies are not easily identifiable at 300 and

600 m; they almost got masked in the low dynamic heights covering most of the gulf (Figure 4.5a). However, anticyclonic eddies (A1 and A2) hugging the southern coast are well identifiable at 300 and 600 m levels. Similarly, the band structure of the geostrophic currents, extending all over the water column (bottom panel) suggest the presence of eddies in the deeper layers. Whereas in February and March, the cyclonic eddy (C3) and the anticyclonic eddies (A1 and A2) seen at the surface extend to 600 m depth level. Similarly, the band structure in the vertical section of geostrophic velocities, also extends to about 1000 m depth (Figure 4.5b and c). Though the eddies extend over most of the water column, the geostrophic velocities associated with these eddies are much weaker than that at the surface (about 1/10 only). During both months, in the deeper regions (300 m and 600 m) the eastward flows along the southern side are stronger than the westward flows in the north.

During April, the geostrophic currents are still similar to the previous winter months (Figure 4.5d). They are embedded with a row of eddies in them. At the western part of the gulf, an anticyclonic eddy (A1) is seen only partly along the northern side due to lack of data. The cyclonic eddy (C3) seen in the center of the gulf at the surface, is not seen at 300 and 600 m. Instead another cyclonic eddy (C4) is seen at 300 and 600 m. This cyclonic eddy as well as the other eddies extend to about 900–1000 m depth as seen in the vertical section of geostrophic velocities shown in the bottom panel of Figure 4.5d.

The geostrophic circulation in May is characterized by the presence of three eddies (C1, A1 and C3) inside the gulf and one outside the gulf in the east (A2). The flows in the east are stronger than those in the west. Unlike the previous months, the flows in the north or south are not unidirectional. The flows switch from westward to eastward depending on their proximity to the eddies. The two cyclonic eddies (C1 and C3) seen at the surface are also seen at 300 and 600 m (Figure 4.5e). The anticyclonic eddy A1 sandwiched between the two cyclonic eddies (C1 and C3) also extends to 300 and 600 m depth levels. The anticyclonic eddy (A2) seen outside the gulf, at the surface, also extends to 600 m.

In the vertical section, most of the alternating bands of northward and southward flows extend from the surface to about 800–1000 m. The flows are strong in the upper 400 m.

In June, the summer monsoon establishes over the Gulf of Aden and northwestern Arabian Sea with eastward geostrophic flows all over the gulf (Figure 4.5f). The anticyclonic eddy (A1), that occupies most of the central region of the gulf at the surface, is seen at 300 and 600 m (Figure 4.5f). The anticyclonic eddy (A2) seen outside the gulf, in the east, also extends to 300 as well as 600 m. So does the cyclonic eddy C4.The vertical section of geostrophic velocities shows that the flows are strong in the upper 400 m.

In July, the pattern is similar to that in June; but the eastward flows at the surface as well as in the deeper layers strengthen further. Effectively, the geostrophic currents appear as meandering flows due to the presence of cyclonic and anticyclonic eddies (Figure 4.5g). The anticyclonic eddy (A1) seen at the surface is also seen in the deeper layers (Figure 4.5g). The eddies, C4 and A2 seen outside the gulf in the east are also seen at deeper layers.

The surface circulation pattern during August is also similar to that of July, with eastward flows all over the gulf. However, the geostrophic currents at 300 and 600 m are in the opposite direction to that at the surface (Figure 4.5h). At 300 m and at 600 m, the flows have reversed and are towards the west in the north and eastward in the south. Outside the gulf the cyclonic eddy (C4) seen at the surface extends to the deeper depths, but the weak anticyclonic eddy (A1) seen at the surface does not show up at deeper depths (Figure 4.5h). However, the alternate bands of geostrophic currents seen in the vertical section presented in the bottom panel indicate the effect of eddies in the deeper layers.

The flow structure in September (Figure 4.5i) is also similar to that in August with eastward flows at the surface and westward (eastward) flows on the northern (southern) sides at 300 m and 600 m. The two anticyclonic eddies (A1 and A2) and the cyclonic eddy (C4) seen at the surface are also seen at 300 and 600 m and beyond.

The vertical structure of the circulation in the Gulf of Aden as seen in the geostrophic

Figure 4.5 (a) Geostrophic currents derived from hydrography during January at surface, 300 m and 600 m levels. The colour shades in the upper three panels represent the dynamic topography (dyn. cm) with reference to 1000 m. The geostrophic currents (north–south) across the section, marked with a line in the upper panels, is also shown in the bottom panel. Different colour scales are used to highlight the presence of eddies.

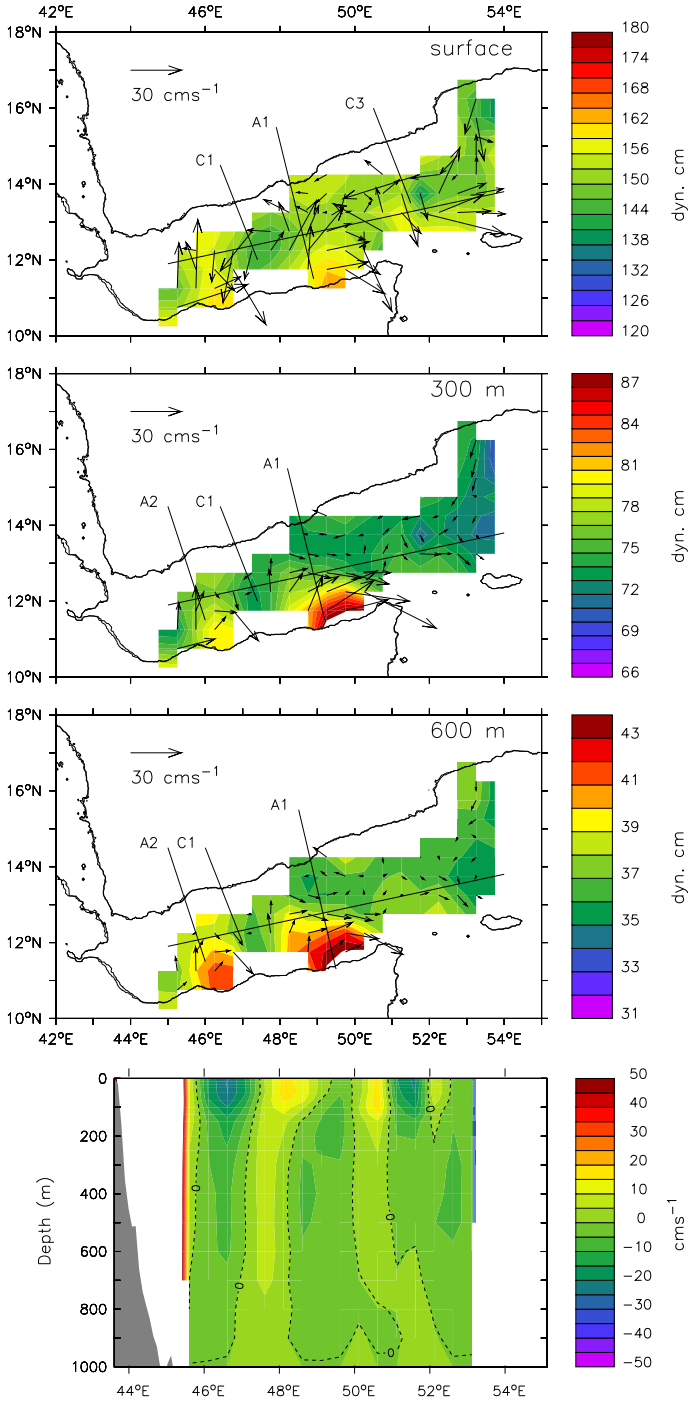

Figure 4.5 (b) Same as for 4.5a, but for the month of February

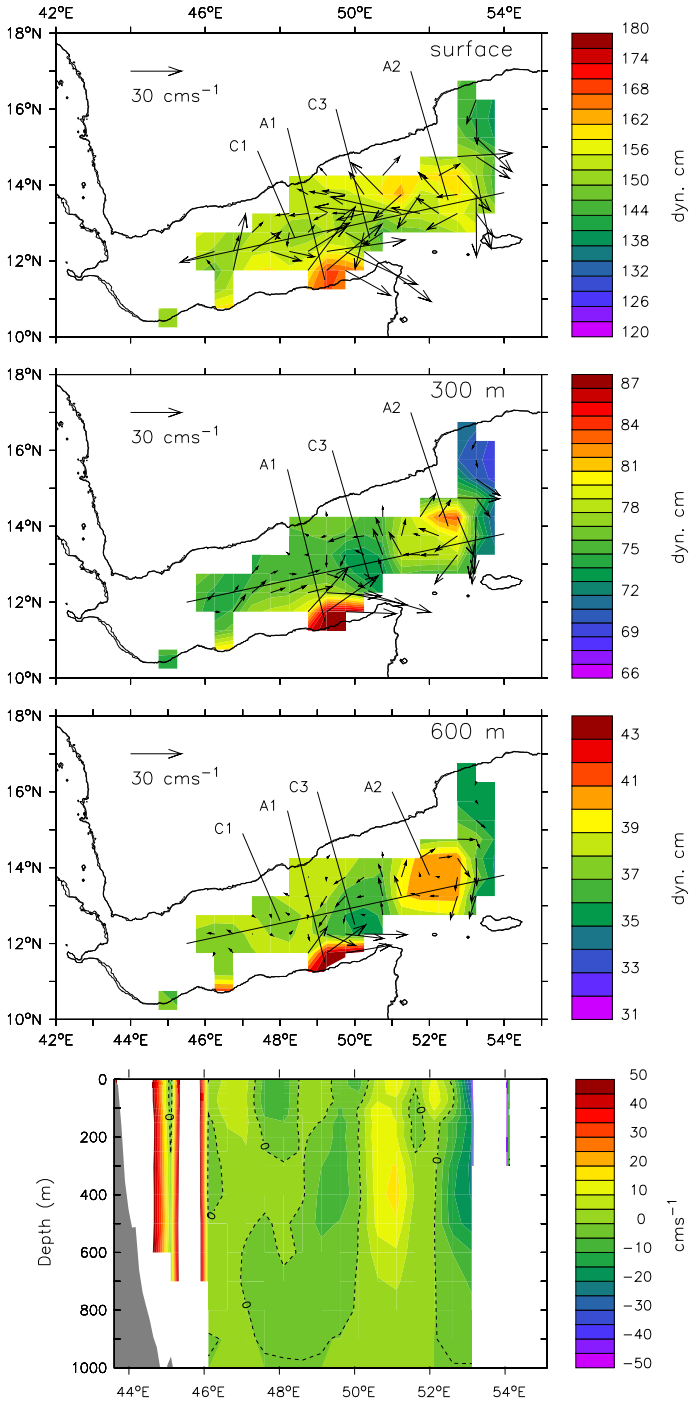

Figure 4.5 (c) Same as for 4.5a, but for the month of March

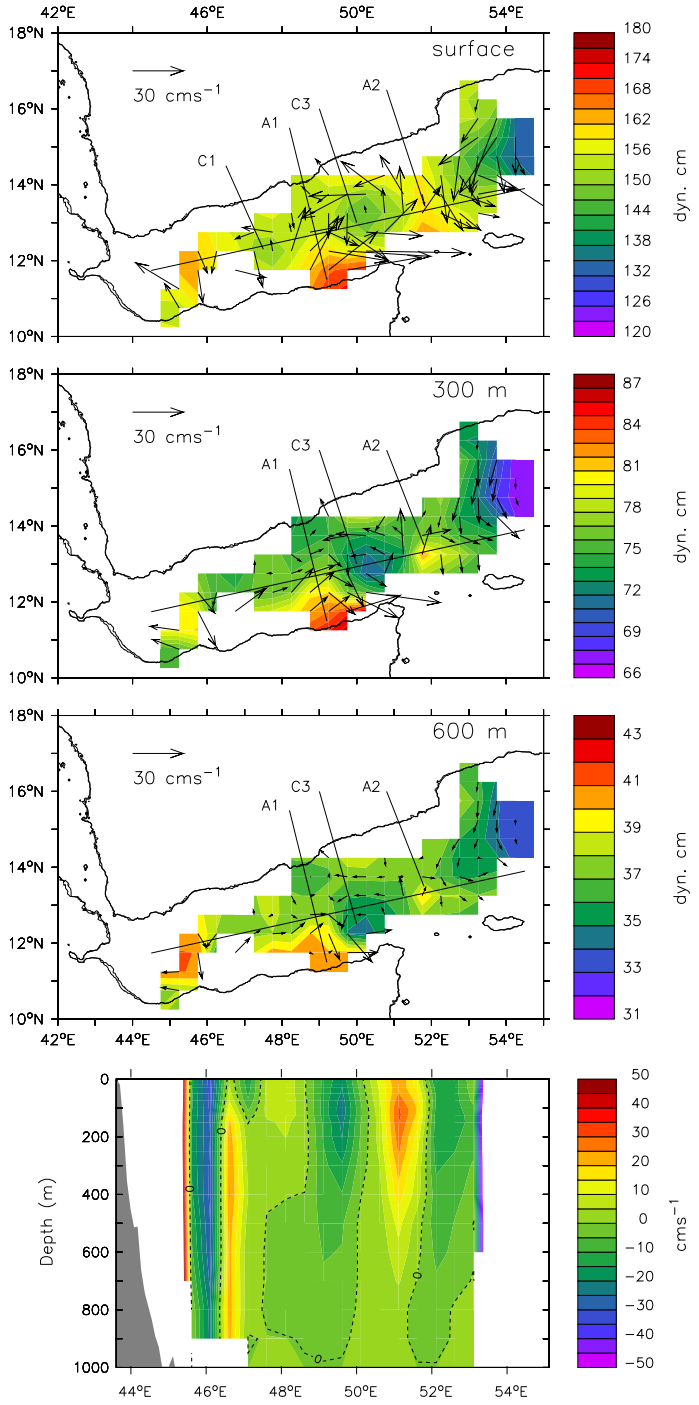

Figure 4.5 (d) Same as for 4.5a, but for the month of April

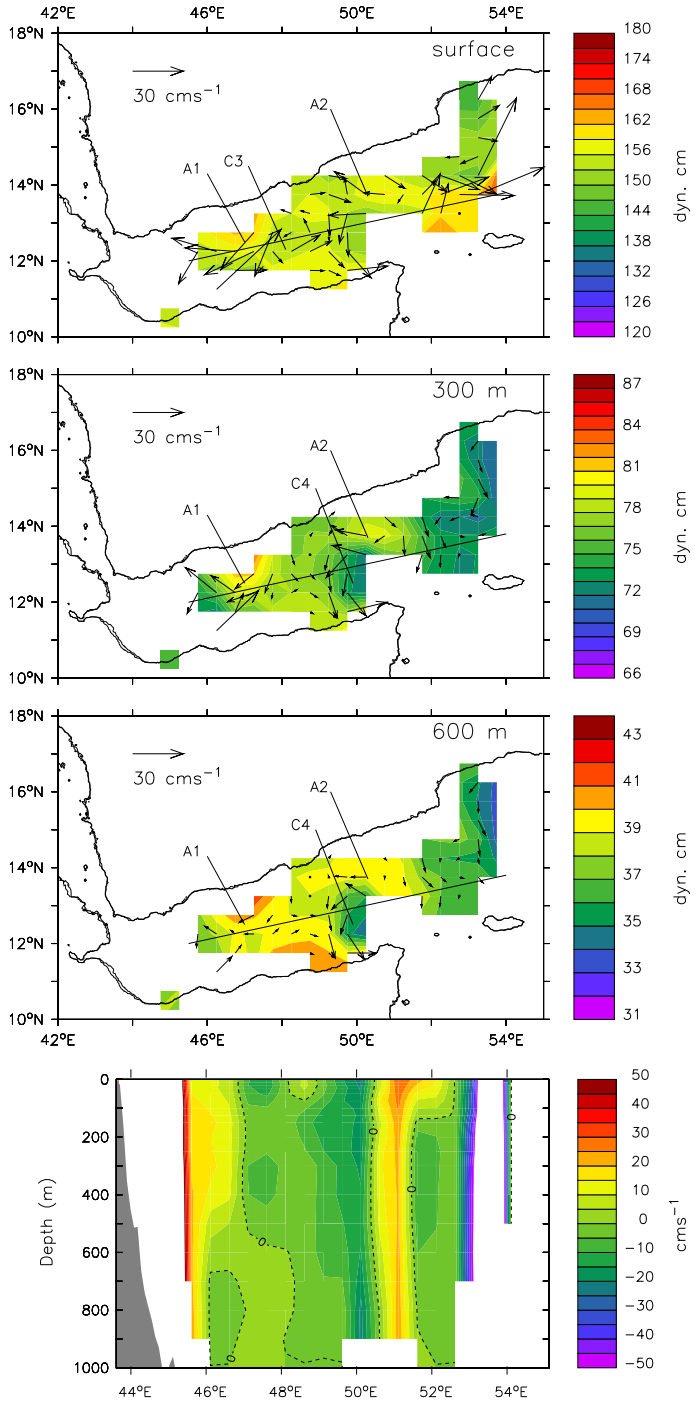

Figure 4.5 (e) Same as for 4.5a, but for the month of May

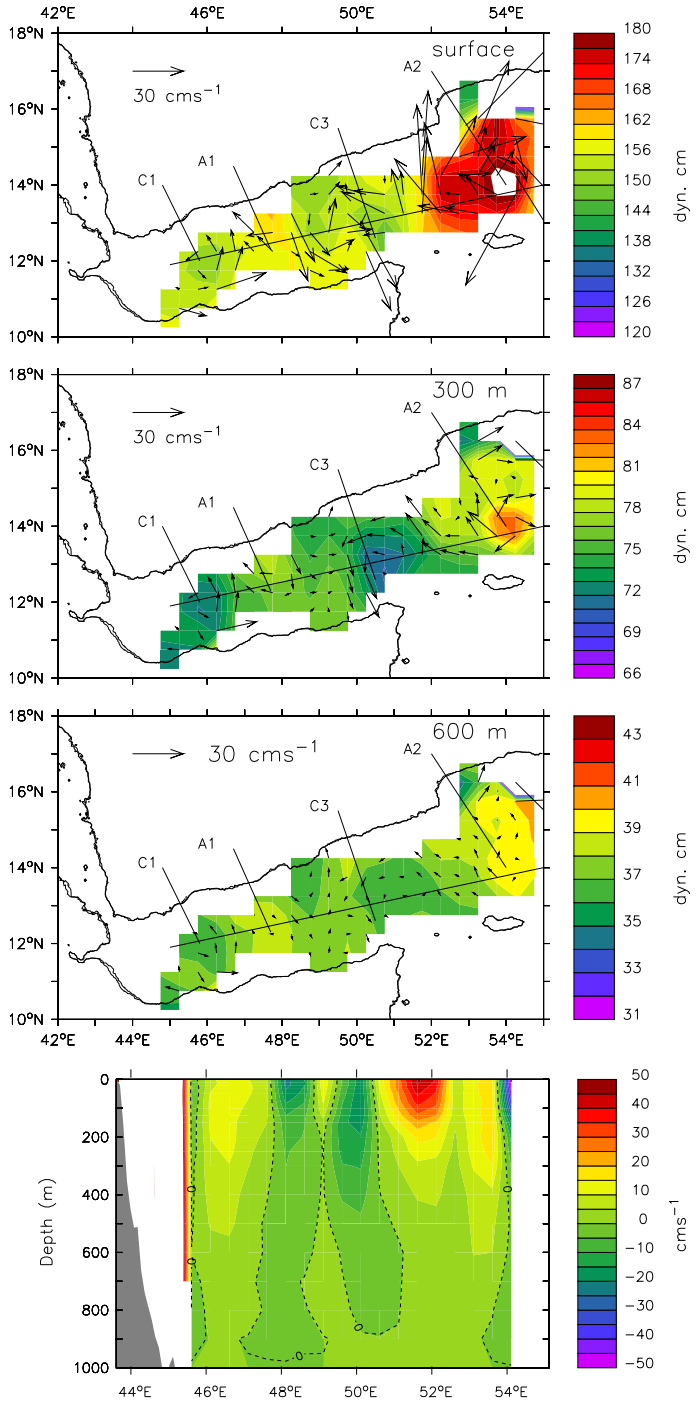

Figure 4.5 (f) Same as for 4.5a, but for the month of June

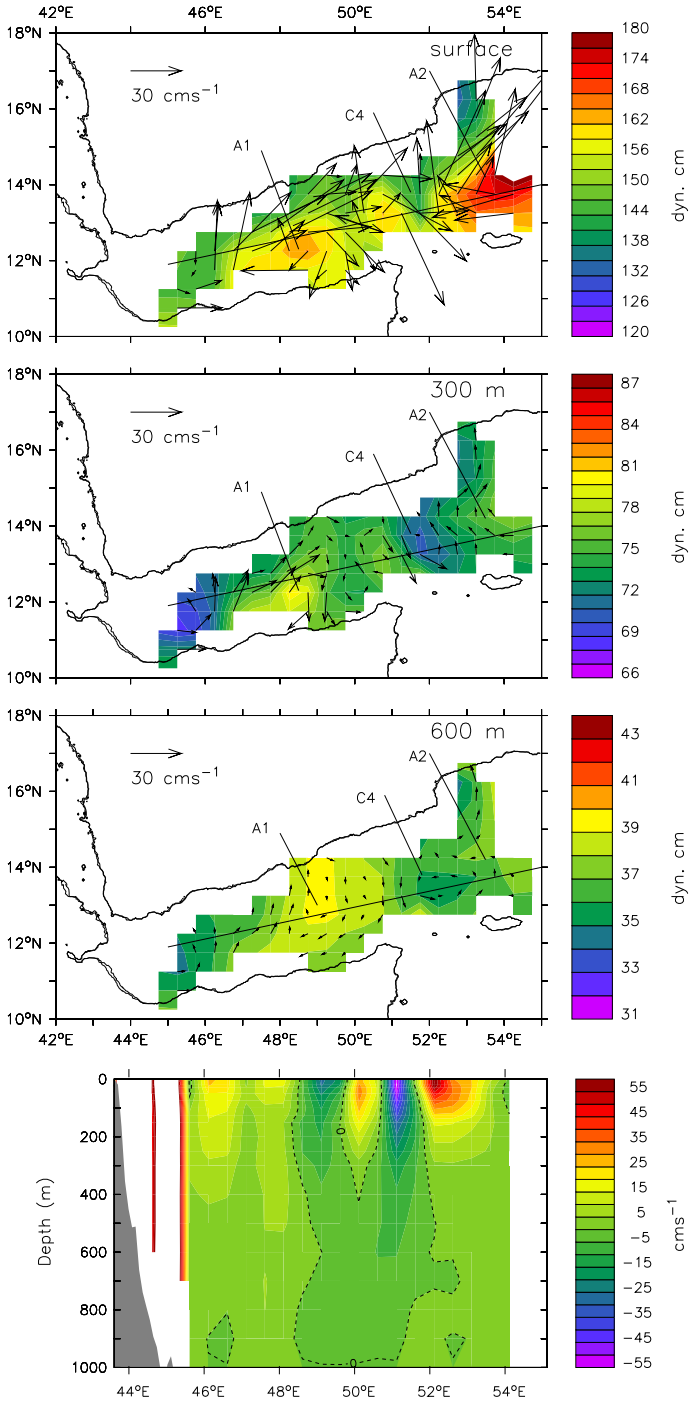

Figure 4.5 (g) Same as for 4.5a, but for the month of July

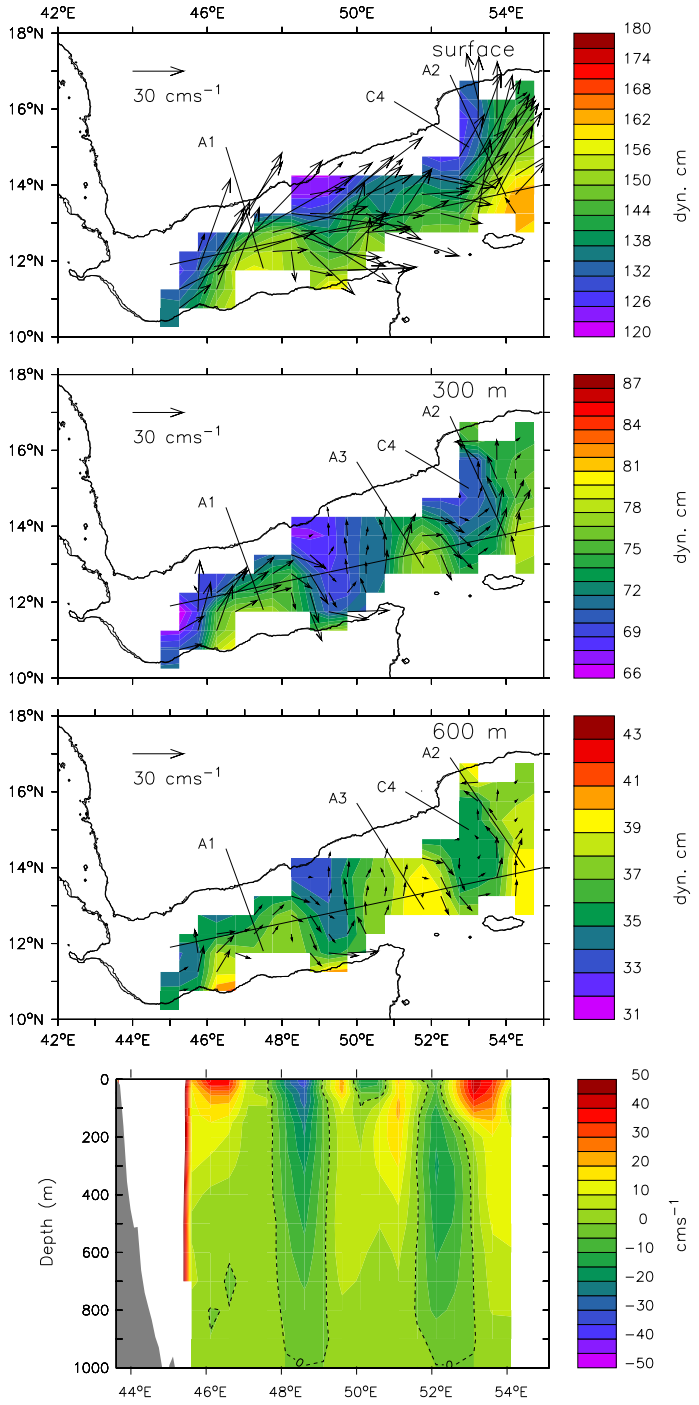

Figure 4.5 (h) Same as for 4.5a, but for the month of August

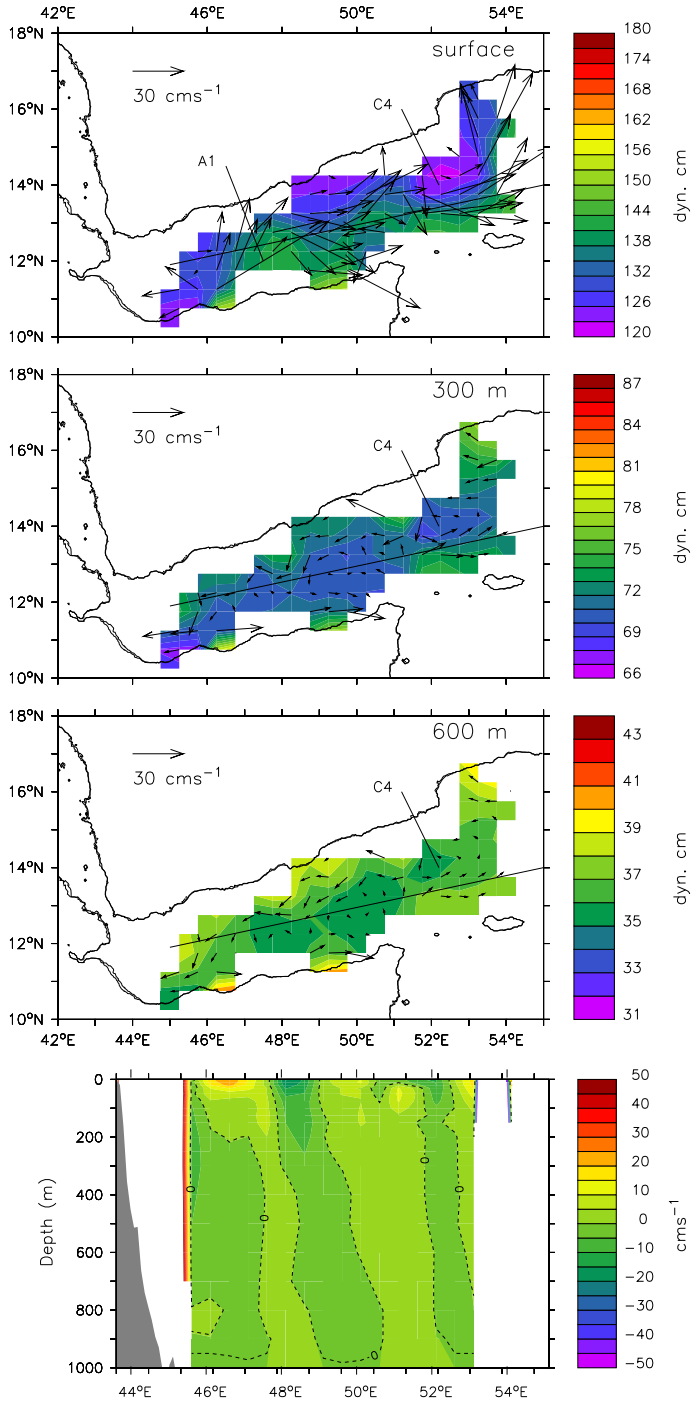

Figure 4.5 (i) Same as for 4.5a, but for the month of September

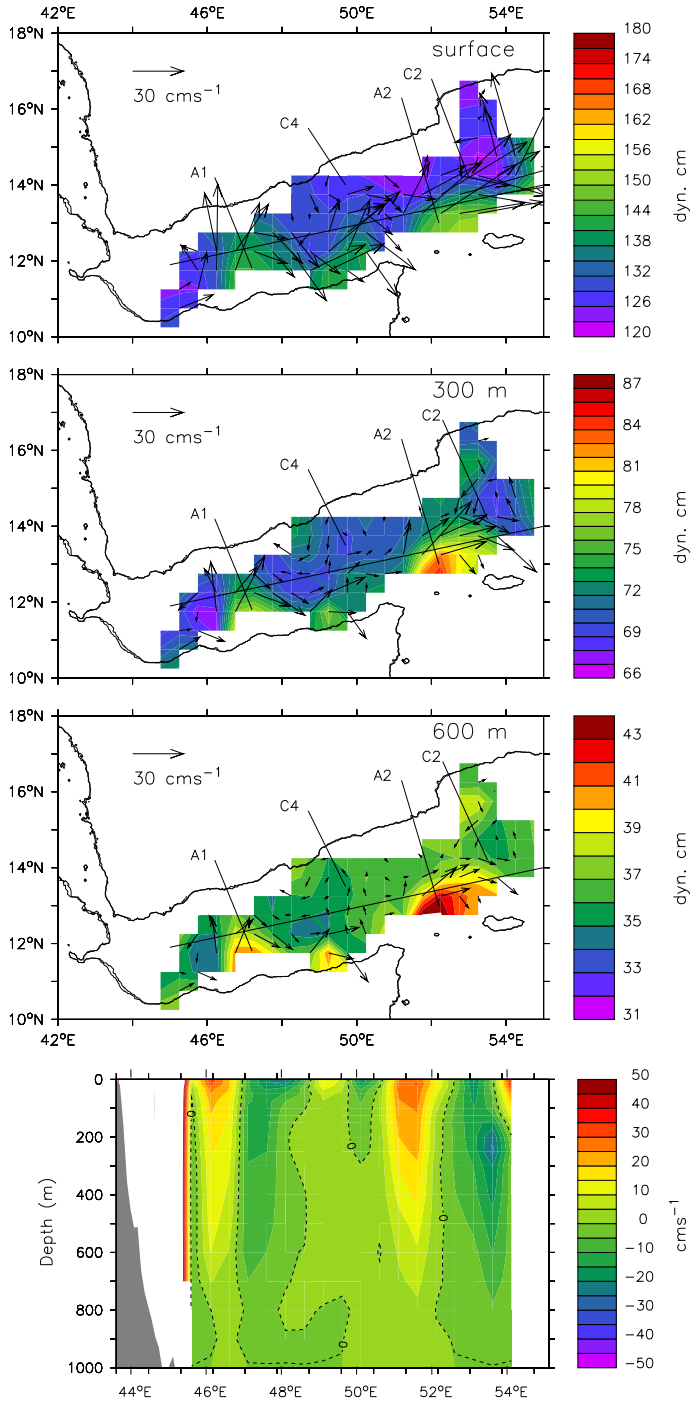

Figure 4.5 (j) Same as for 4.5a, but for the month of October

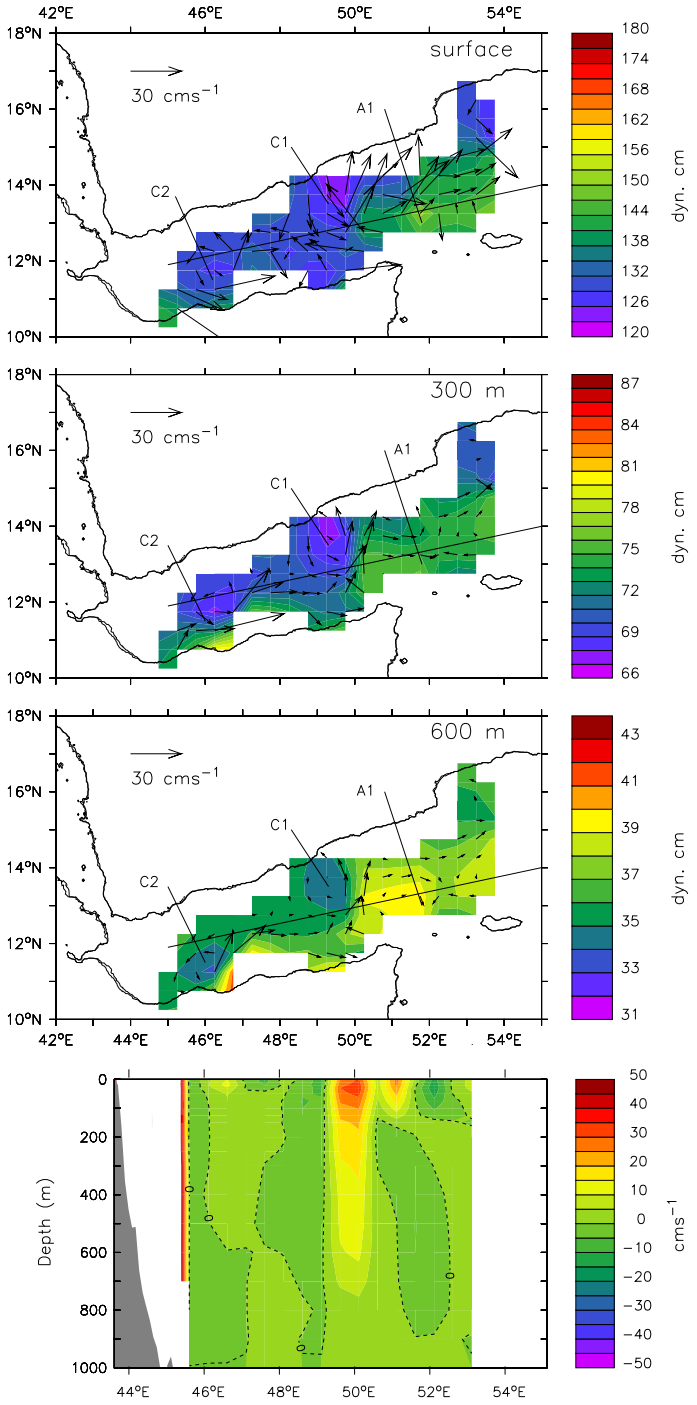

Figure 4.5 (k) Same as for 4.5a, but for the month of November

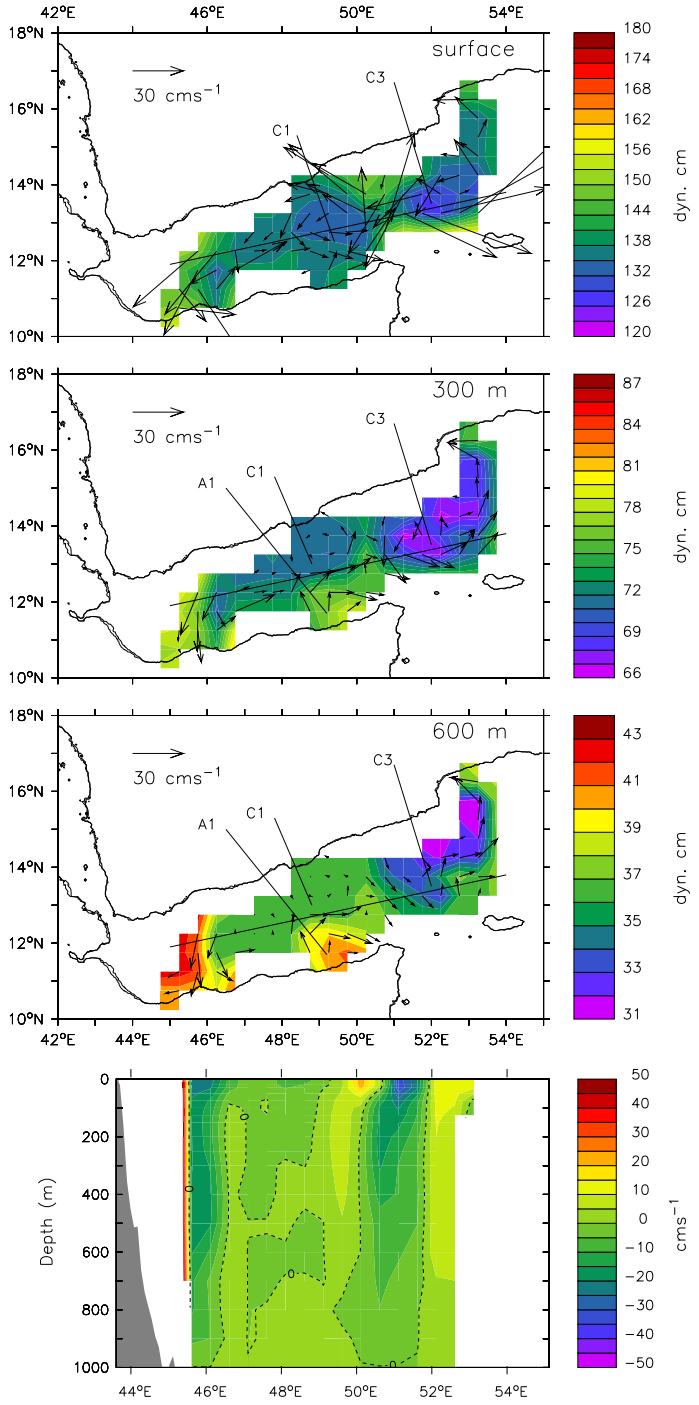

Figure 4.5 (l) Same as for 4.5a, but for the month of December

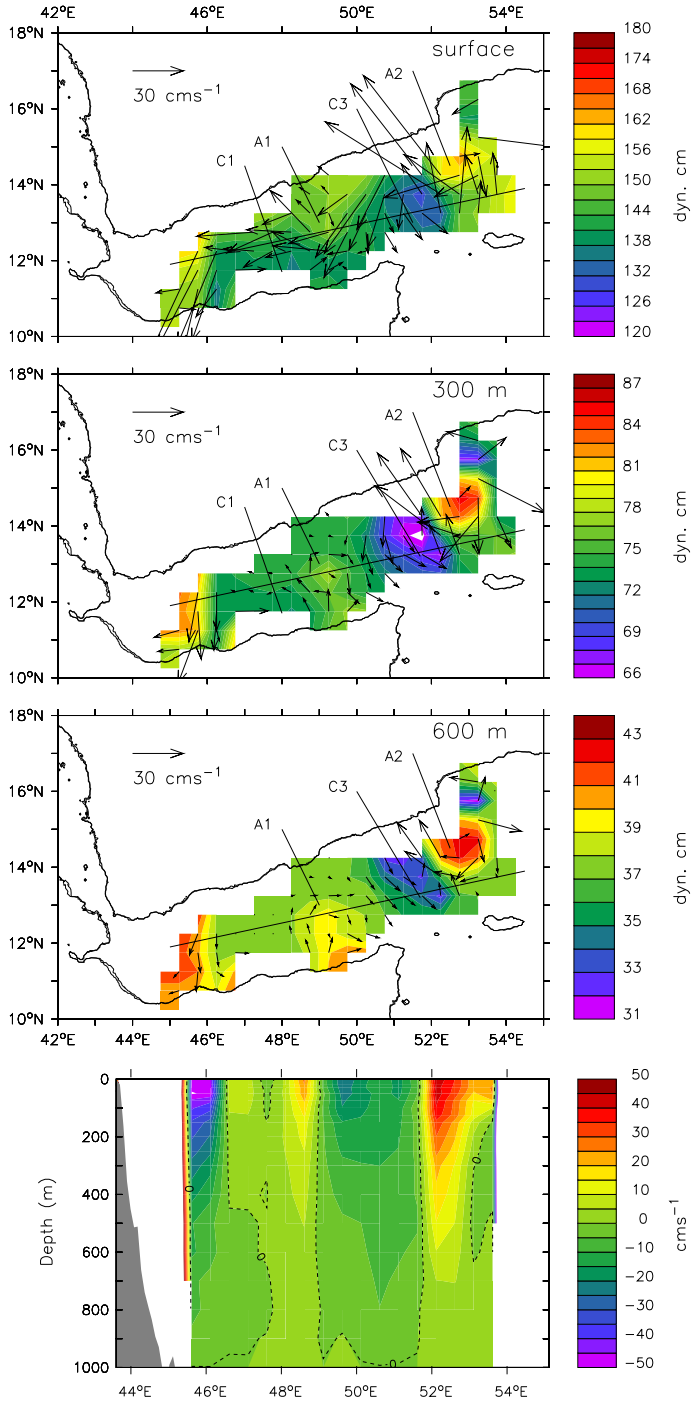

currents derived from hydrographic data are highly influenced by a row of eddies embedded in them. From the analysis, presented here, it is clear that the eddies seen at the surface, in hydrography as well as in the altimeter derived SLA, extend to deeper depths, often to 1000 m. During most of the months, the flows across the water column are unidirectional, except during August-September, when they show a partial reversal on the northern side. Here, the flows are toward the east at the surface and are toward the west at 300 and 600 m. In general, eastward flows exist across the water column during the summer monsoon (June–September) and westward flows exist in the winter monsoon (November–February). The flows during October as well as in March–April resemble the winter pattern. The flow directions during May, however, do not coincide with either the summer or winter monsoon patterns. They are highly cellular under the influence of eddies.

4.4 Interannual variability in the surface currents

Having analyzed the evolution of currents at the surface and in the deeper layers of the Gulf of Aden using the climatology of ship drifts, Ekman drifts, hydrography and altimeter derived SLA, in this section, we present the interannual variability of sea level as a proxy to the variability of geostrophic currents at the surface. For this purpose, the merged altimeter SLA for 11 years during the period 1993 to 2003 are used because that is the only data set available to carry out the analysis of interannual variability. The 11 year long SLA time series is a combination of signals with different time scales. The least resolved periodicity is determined by the repeat period of satellites and the largest resolved periodicity is determined by the length of the series. This implies that this series can resolve signals on the time scales from weeks to a few years (interannual scales).

Several techniques are available to resolve the signals at different periodicities hidden in a time series. Here, we use the wavelets to resolve the variabilities in SLA at different

time scales because that determines the dominant modes of variability and its variability in time. The wavelet technique has wide application in geophysical time series analysis [Foufoula-Georgiou and Kumar, 1995].

To determine the dominant modes of variability in the SLA time series we have used the Morlet wavelet described in Torrence and Compo [1998]. This method allowed us to estimate the wavelet power due to the variability in SLA at different periods ranging from high–frequency (2 weeks) to interannual (5 years) periods. To describe the spatial distribution of the variability in SLA time series, first, we have estimated wavelet power at each grid point of altimeter SLA. Figure 4.6a shows the wavelets at 5 locations, 2 inside the gulf and 3 in the northwestern Arabian Sea adjacent to the gulf. The wavelets significant at 95 and 99% confidence levels are also shown in Figure 4.6b and c. The annual and high–frequency signals were significant inside and outside the gulf, while the interannual signal was not significant inside the gulf (Figure 4.6). These wavelet powers, obtained at each grid point, were averaged over five frequency bands, namely, high-frequency (0.0333-0.00365 cycles per day or periods of 30-274 days), annual (0.00307-000258 cycles per day or 325-388 days) and three interannual bands namely biannual (0.00184–0.00129 cycles per day or 548–776 days), tri-annual (0.00108–0.00091 cycles per day or 922–1097 days) and quad–annual (0.00077–0.00064 cycles per day or 1305–1552 days) in time to represent the spatial variability as shown in Figure 4.7. Essentially, the wavelet power in the high–frequency band represents the magnitude of SLA oscillations at periods less than an year and the wavelet power in the annual band represents the magnitude of SLA oscillations at periods of around 1 year. Similarly, the wavelet power in the interannual band represents the oscillations in SLA at 18 months or more. The spatial variability shown in the middle and right columns of Figure 4.7 represents the averaged wavelet powers significant at 95% and 99% levels respectively.

As expected, the wavelet power in the SLA time series is highest ($> 2^{10}$ cm^2) and significant at 95 as well as 99% confidence levels in the annual band everywhere in the

Figure 4.6 (a) Time-scale representation of the wavelet powers spectrum (log scale) of the time sesies of altimeter derived SLA at the grid points centered at 46° E, 12° N (1), 50° E, 13° N (2), 53° E, 8° N (3), 53° E, 10° N (4), and 53° E, 14° N (5). Morlet wave transform was used to compute the wavelets using 11 years weekly spaced data set. The cone of influence aso is shown (the curved line). Wavelets having periods > 1300 days are not acceptable during any time.

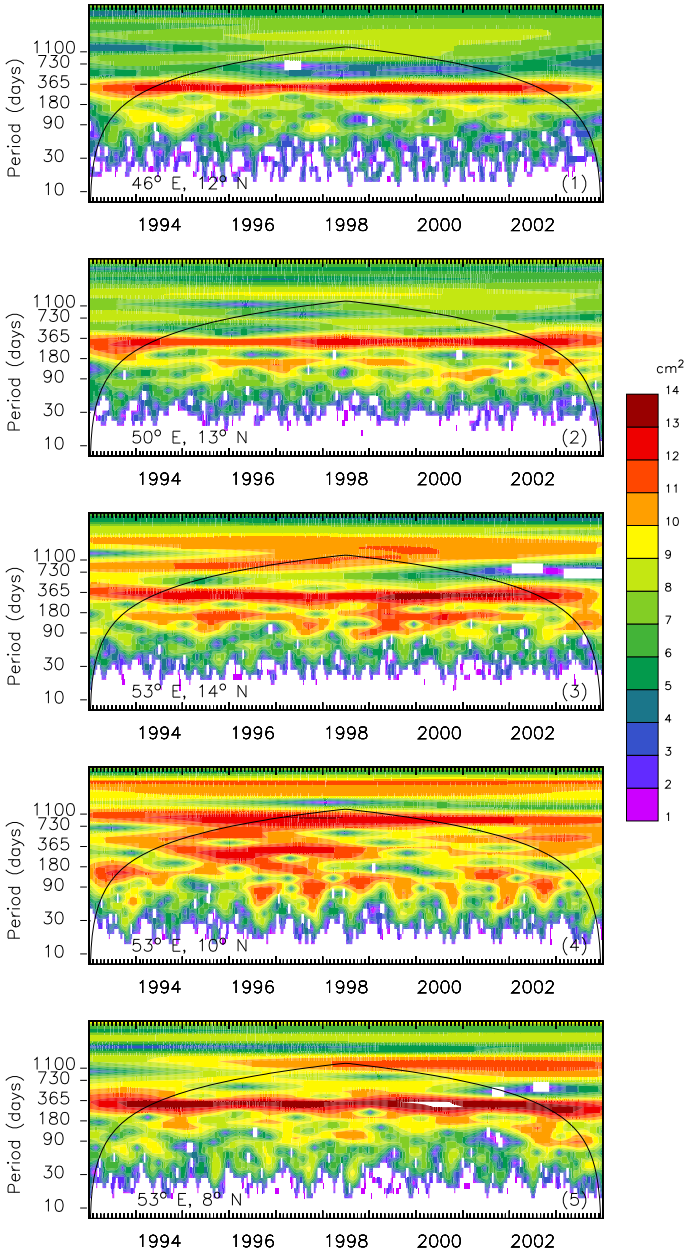

Figure 4.6 (b) same as 4.6a for confidence level at 95%

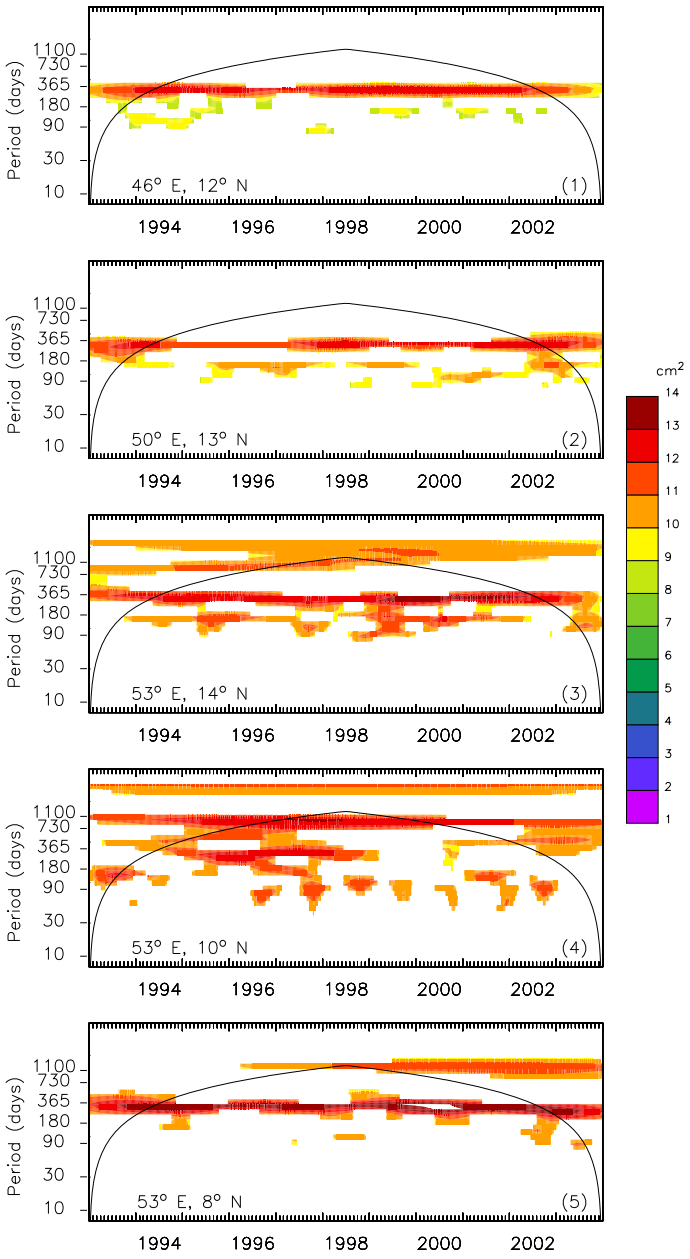

Figure 4.6 (c) same as 4.6a for confidence level at 99%

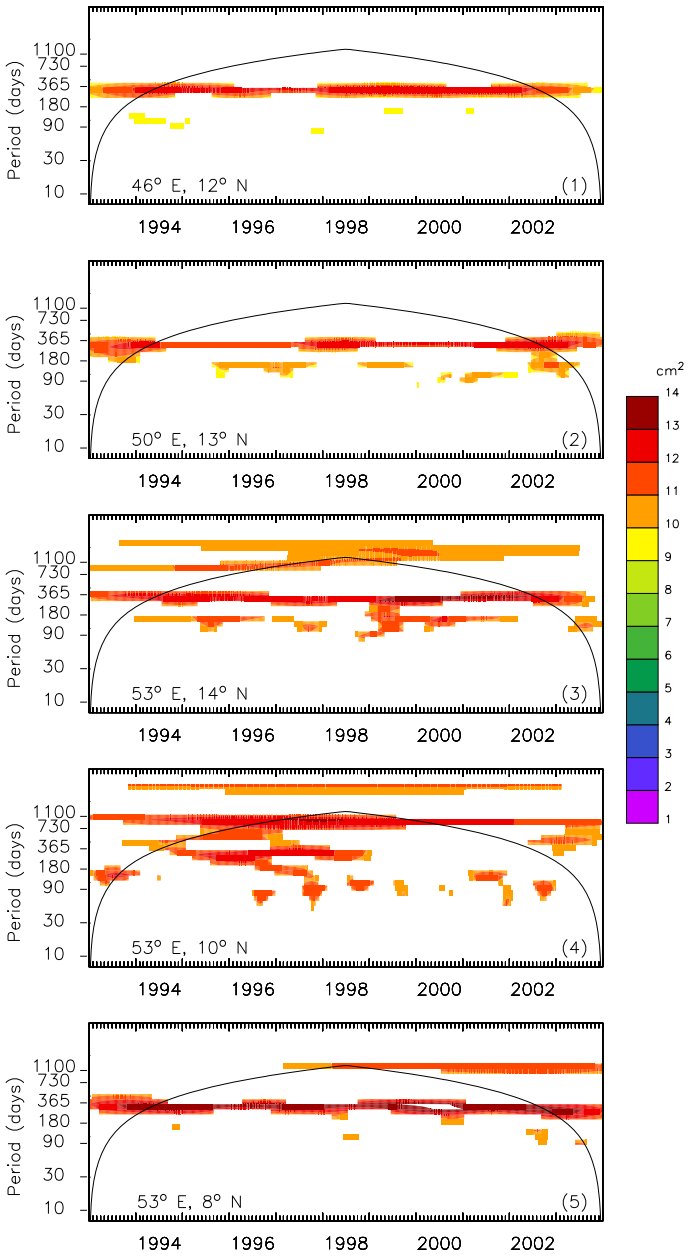

gulf as well as over most of the northwestern Arabian Sea (Figure 4.7). It is highest in the Somali eddy region (2^{13} cm^2), southern Red Sea (2^{12} cm^2) and in the Gulf of Aden (2^{11}–2^{12} cm^2). Comparatively, wavelet powers are higher in the northern half of the Gulf of Aden (2^{12} cm^2) than in the southern half (2^{11} cm^2). The wavelet power in the western most part of gulf (west of 46° E) is also $> 2^{12}$ cm^2. Compared to the wavelet power contained in the annual frequency band, it is lower in the other bands, the high–frequency (30–274 days) and interannual bands (545–1552 days). In the high–frequency band, it is $< 2^7$ cm^2 in the Gulf of Aden and it is $\sim 2^8$ cm^2 in the Somali eddy region and at the entrance to the gulf; it is low (2^6–2^7) in the western gulf (west of 48° E).

The power is least in the Gulf of Aden in all three interannual bands ($< 2^6$ cm^2). Further, it is significant only over small patches in the central gulf at 95 % confidence level in tri–annual bands. However, they are not significant at 99% confidence level (Figure 4.7) inside the gulf in all three interannual bands though they are still significant in the adjoining northwestern Arabian Sea, especially at the entrance to the gulf. This implies that the SLA variability in the Gulf of Aden is insignificant at interannual frequencies. The same will be true in the case of surface geostrophic currents because they are tightly linked to the slope of SLA.

4.5 Discussion

Three major data sets have been used to describe the monthly evolution of currents in the Gulf of Aden. They consisted of a new climatology of hydrography, satellite altimeter derived SLA, and the climatology of ship drifts. The QuikSCAT derived winds were used to estimate the Ekman drifts. The three data sets together with the Ekman drifts were consistent with each other and brought out the salient features of seasonal cycle of circulation in the Gulf of Aden.

The analysis of circulation in the Gulf of Aden presented here not only confirmed

Figure 4.7 Horizontal distribution of the 11 years (1993–2003) averaged wavelet powers spectrum (log scale) of the time sesies of altimeter derived SLA for different bands. Morlet wave transform was used to compute the wavelets using 11 years weekly spaced data set.

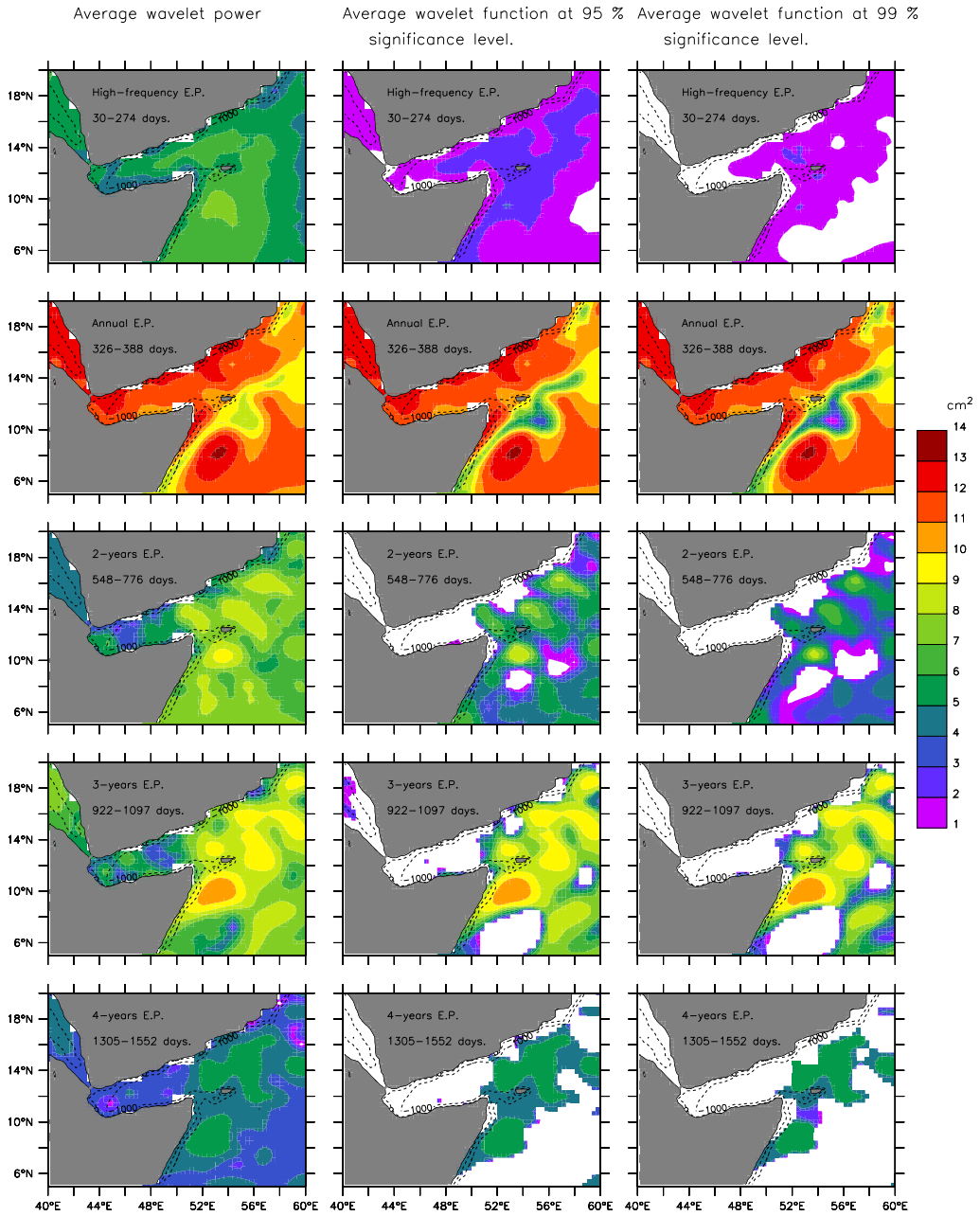

the earlier descriptions on the seasonality of surface currents but also provided new insights. First and foremost is that the currents in the Gulf of Aden are not so simple as thought earlier; they are complicated by the presence of eddies embedded in them. Second, the eddies influenced the flows during all months. Third, the eddies are found only in geostrophic currents and not in Ekman drifts induced by winds and fourth, the eddies act over the entire water column extending from the surface to at least 1000 m.

Due to the presence of eddies, the flow directions in the north often differed from the south. The previous studies [Mohammed and Kolli, 1992; Kolli et al., 1992] that described the circulation in the Gulf of Aden failed to capture the opposite flows in the south because of lack of data from the southern part. The data set used by Mohammed and Kolli [1992] did not extent towards the south; also, it was restricted to just three months (January, May and August). Mohammed and Kolli [1992] and Kolli et al. [1992] presented the circulation for January, May and August based on the dynamic topography (0/500) derived from hydrographic data. During May, they observed weak flows and a clockwise (anticyclonic) cell in the eastern gulf. Our analysis using hydrography and altimeter SLA showed the existence of an anticyclonic cell (A2) in the east and also the two additional cells inside the gulf (Figure 4.3e). During January, they reported an anticlockwise (cyclonic) cell in the central gulf (between 46–50° E). This cell (C1) is seen in our analysis also (Figure 4.3a). But in addition to this cell, our analysis also showed another anticyclonic cell (A1) inside the gulf in both data sets. Mohammed and Kolli [1992] observed that in August, the anticlockwise (cyclonic) cell in the central gulf got replaced with a clockwise (anticyclonic) cell. This is true of our analysis also (Figure 4.3h).

The ship drift data showed the seasonality in the circulation (Figure 4.1) similar to other data sets, but cannot be used to bring out the mesoscale eddies embedded in the flows. Similarly, the Ekman drifts estimated from winds (Figure 4.2) also did not show the presence of eddies in the gulf or adjoining seas. Ekman drifts were towards the west during the winter monsoon (November–March) and towards the east during the summer

monsoon (June–August). The Ekman flows in the month of September appeared to be an exception to the summer monsoon flow pattern; the flows inside the gulf were abysmally weak (Figure 4.2i). The case was similar in May, the transition period between winter and summer monsoons. The Ekman drifts in April as well as in October, the other two transition months, were westward similar to the winter flows. Thus, due to the Ekman drifts, two well defined flow patterns form in the Gulf of Aden; (i) a westward flowing winter pattern and (ii) an eastward flowing summer pattern. The winter pattern started in October and continued till April. Whereas the summer pattern existed only for a short duration of 3 months (June–August). In addition to the generation of well defined flow patterns, the Ekman drifts do not seem to contribute to the generation of eddies in the gulf.

The analysis of geostrophic currents, however, presented the embedded eddies in the flows (Figure 4.3). Several eddies were seen in the geostrophic currents during all the months and they were consistent in the geostrophic currents derived from hydrography and altimeter SLA. As seen in the net surface flows shown in Figure 4.4 the eddies dominated the circulation in the Gulf of Aden over the mean flow. Due to the importance of eddies in the circulation of the Gulf of Aden, a separate chapter (Chapter 5) has been dedicated to further analyse the characteristics of eddies and their origin.

The net flows at the surface in the western gulf are towards the Red Sea during October–April and is at its maximum during November to February. This westward flow would transport water from the Gulf of Aden into the Red Sea. Maillard and Soliman [1986] reported the mean salinity and temperature of this water entering the Red Sea through Bab el Mandab as 36.5 psu and 25 °C. Al Saafani and Shenoi [2004] identified this water with a temperature varying between 27.0 and 28.0 °C and salinity between 36.5 and 37.0 psu during the winter of 1996. The eastward flows in the western end of the gulf in the summer monsoon (June–August) (Figure 4.4g and h) are consistent with the outward flow from the Red Sea in the surface layer [Neumann and McGill, 1962;

Patzert, 1974; Murray and Johns, 1997; Al Saafani and Shenoi, 2004]. Similarly, the westward geostrophic currents in the western end of gulf at 300 and 600 m layers in August–September (Figure 4.5h, i) are consistent with the intrusion of Gulf of Aden water into the Red Sea in the intermediate layers reported by Murray and Johns [1997] and Al Saafani and Shenoi [2004]. Murray and Johns [1997] reported that the summer regime in the Bab el Mandab Strait is dominated by the massive intrusion of cold (19 °C) low salinity (36.0–36.5 psu) water from the Gulf of Aden. They estimated its presence in the water column as high as 70% during July to early September in 1995.

The eddies seen at the surface extend to deeper layers, often to 1000 m or more. Due to the non–availability of direct measurements of currents across the water column, we have to restrict the analysis of vertical structure of currents to the geostrophic currents estimated from hydrography. Our analysis showed a well developed anticyclonic eddy (A1) and a cyclonic eddy (C1) on its west inside the gulf during winter monsoon in the geostrophic currents derived from hydrography and altimeter SLA (Figure 4.3a and b). It reached as deep as 1000 m (Figure 4.5a and b). Bower et al. [2002] found these eddies in the in situ measurements of currents across the water column during February–March 2001. They recorded these eddies at 100, 300 and 600 m and denoted them as A1 and C2 (C1 in our analysis). They also reported another cyclonic eddy, C1, centered at 44.5° E, west of C2. This eddy was not captured in our analysis because the geostrophic currents were estimated with reference to 1000 m depth and the region west of 45° E is shallower than 1000 m. Bower et al. [2002, 2005] have highlighted the importance of these eddies on the spreading rates and pathways of Red Sea water in the Gulf of Aden between 400–800 m.

The annual and high-frequency signals dominate the sea level variability in the Gulf of Aden (Figures 4.6 and 4.7). The SLA variability in the gulf at interannual frequency is minimum and insignificant at 99% confidence level. It is significant at 95% confidence level only over small patches inside the gulf (Figure 4.7). Since the variability in SLA is

related to the geostrophic currents at the surface, it is clear that the interannual variability in the surface geostrophic currents inside the gulf are also insignificant. The geostrophic currents have dominated the net surface flows as seen in Figure 4.4 in the Gulf of Aden. Hence, it would imply that the observed variability (as depicted by the power of wavelets) in the SLA in the five bands depicts the variability of circulation. Based on this argument, we may conclude that the interannual variabilities in the circulation in the Gulf of Aden are lower (and insignificant) than that at annual and higher frequency bands.